REFERENCE ONLY
HAWAII INSTITUTE OF GEOPHYSICS
LIBRARY ROOM

THESIS
GEO
Sto
Che
MS

CHEMISTRY, PETROGRAPHY, AND HYDROTHERMAL ALTERATION OF BASALTS FROM HAWAII GEOTHERMAL PROJECT WELL-A, KILAUEA, HAWAII

A THESIS SUBMITTED TO THE GRADUATE DIVISION OF THE
UNIVERSITY OF HAWAII IN PARTIAL FULFILLMENT
OF THE REQUIREMENTS FOR THE DEGREE OF

MASTER OF SCIENCE

IN GEOLOGY AND GEOPHYSICS

MAY 1977

By

Claudia Stone

Thesis Committee:

G. A. Macdonald, Chairman
Kost A. Pankiwskyj
Ralph Moberly
P. F. Fan

We certify that we have read this thesis and that in our opinion it is satisfactory in scope and quality as a thesis for the degree of Master of Science in Geology and Geophysics.

THESIS COMMITTEE

Gordon P. Macdonald
Chairman

Mark Moberly

Most A. Hammersley

Tom Young Fan

ABSTRACT

A successful 1962 m geothermal test well was drilled in the east rift zone of Kilauea volcano on the island of Hawaii in early 1976. Cores and cutting chips have been analysed chemically, petrographically, and by X-ray diffraction for hydrothermal alteration products.

All of the lavas are quartz-normative tholeiitic basalts. Although scatter is pronounced, plots of oxides vs. depth in the well show that a decrease occurs in SiO_2, FeO, Na_2O, K_2O, MnO, P_2O_5, and TiO_2; an increase is noted in CaO, MgO, and Fe_2O_3. Cu is uniform below 500 m and Cr shows no trend. Most of these observed trends do not agree satisfactorily with leaching and enrichment patterns which should be seen if changes in chemical composition are due to basalt-sea water interaction. MgO variation diagrams show a negative correlation for most oxides. Total FeO and Al_2O_3 are invariant and CaO is covariant. These changes may possibly reflect differentiation of the source region with time, or differentiation of "batches" of magma periodically injected into the east rift zone which could account for the scatter. However, without probe analyses or normalizing the data to Al_2O_3, possible leaching and enrichment effects of groundwater and thermal fluids cannot be dismissed.

Thin sections reveal basalts with phenocrysts of olivine, less than six per cent maximum, and clinopyroxene and plagioclase (An_{75-80}), generally less than one per cent each. Texture is mainly intersertal; intergranular and glassy are not uncommon. Vesicularity ranges from moderate to high (30 per cent) in the upper 875 m of the well; and low to absent in the lower portion. Based on filled vs. unfilled fractures and vesicles, three zones of permeability can be identified: 0-875 m,

highly permeable; 1113-1835 m, poorly permeable; core 10 at 1962 m, moderately permeable.

Beneath a zone of unaltered lavas, high temperatures and thermal fluids have created three zones of altered lavas, each marked by the dominance of a particular mineral. The uppermost altered zone, 675-1300 m, is characterized by montmorillonite with minor calcite, quartz, zeolites, and chlorite. The second zone, 1350-1894 m, is dominated by chlorite with accessory quartz, actinolite, and montmorillonite. The third zone of alteration is observed beginning in core 9, 1984 m, and is pronounced in core 10, 1959 m. Actinolite is the dominant mineral; chlorite, quartz, and albite are accessory alteration products. The mineral assemblage in core 10 resembles that found in greenschist metamorphism.

The changeover temperature from a montmorillonite to a chlorite zone is greater than that found in Icelandic geothermal wells for the same transition. Possibly more acidic water, rock permeability and/or glass content are more significant in the alteration of HGP-A lavas than they are in the alteration of Icelandic basalts.

TABLE OF CONTENTS

LIST OF TABLES

LIST OF ILLUSTRATIONS

INTRODUCTION

A successful, 1962 m geothermal test well, designated Hawaii Geothermal Project Well-A, was drilled in the east rift zone of Kilauea Volcano on the Island of Hawaii (Fig. 1) in early 1976. The elevation at the drill site is about 205 m above sea level which means that the well penetrated a 1747 m sequence of volcanic rocks below sea level, the deepest well yet in the Hawaiian Islands. The success of the well is unusual in that most active geothermal fields are confined to or associated with rocks of a more silicic nature (Berman, 1975). Even in Iceland, silicic volcanism occurs at or near all geothermal fields except the 30 km zone from Reykjanes to Krysuvik (Koenig, 1973).

Above the 207 m level in the well (all references to depth are measured from the surface elevation at the drill site), poor circulation of drilling mud prevented systematic sampling of cutting chips; below that level 780 cutting samples were recovered at 3 to 1.5 m intervals to the bottom of the well. Ten cores totaling 28 m were taken at intervals of 125 to 275 m.

Daniel B. Palmiter, geologist in charge at the site during the drilling operation, macroscopically examined the cutting chips for percentages of vesicularity, black glass and alteration products. From these he interpreted that the well penetrated a sequence of thin subaerial pahoehoe and aa basalt flows and submarine pillow basalts, with a zone of intense hydrothermal alteration beginning about 1350 m and continuing to the bottom of the well (D. Palmiter, personal communication, 1977). Microscopic examination of cores and cuttings, X-ray diffraction analyses of hydrothermal alteration products, and major and trace element analyses were carried out by the writer.

Figure 1. Map of the island of Hawaii (from Macdonald and Abbott, 1970) showing the location of Hawaii Geothermal Project Well-A, closed circle; proposed summit of Kulani Shield, open circle; and proposed summit of Ninole Shield, open square (G.A. Macdonald, personal communication, 1977).

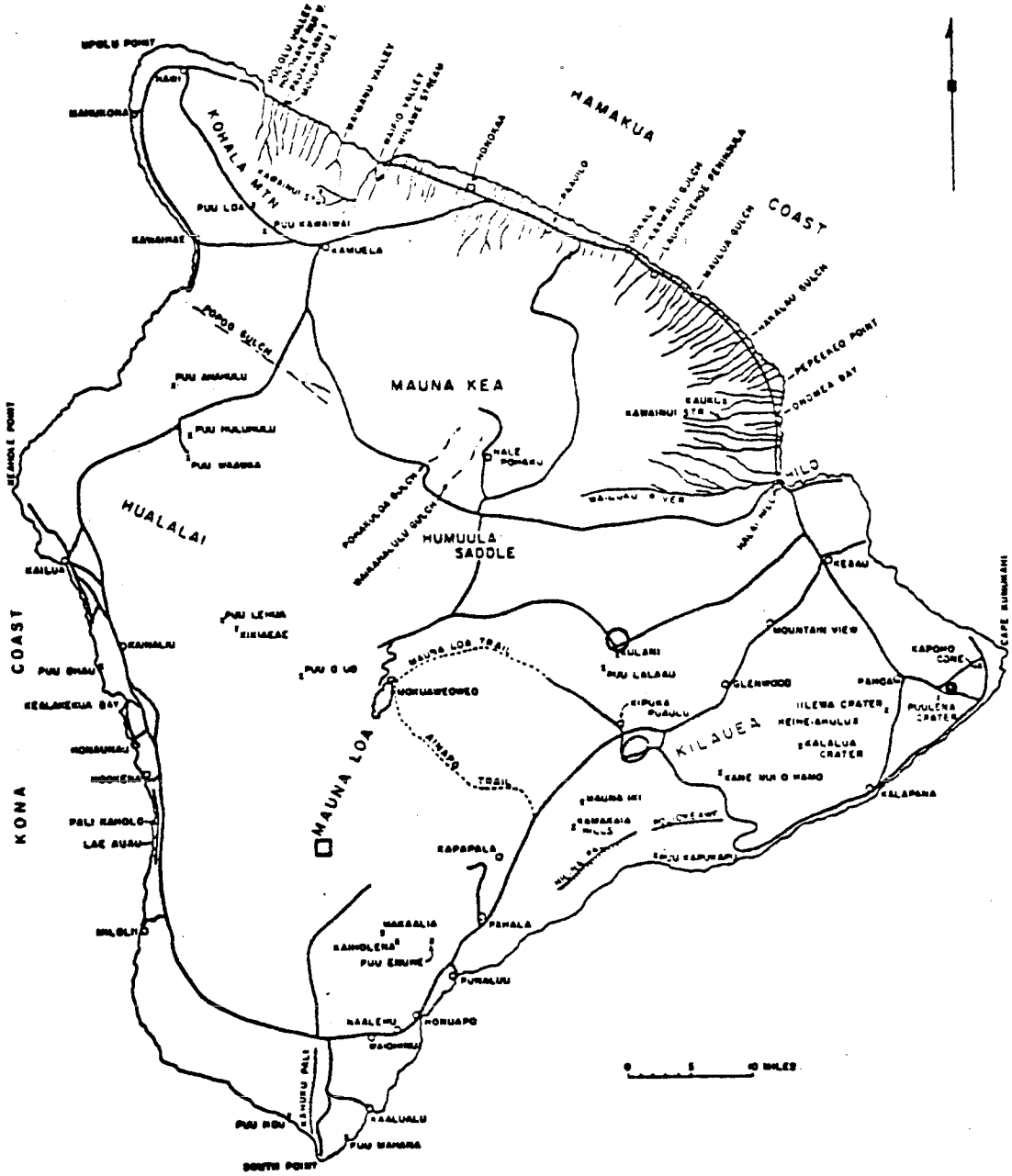
HAMAKUA
COAST
KOHALA MTN
MAUNA KEA
HUALALAI
HUMUULA SADDLE
MAUNA LOA
KILAUEA
KONA
COAST
HILO
PUU LOA
KAMUELA
HAKALAU
KEAUHOU
KAILUA
KEALAKEKUA BAY
KEALAKEKUA
KAWAIHAE
MOUNTAIN VIEW
GLENWOOD
PAHOA
KAPOHO CORE
PUULENA CRATER
HILEWA CRATER
HEIHE-BAULUS
KALALUA CRATER
KALAPANA
KAPAPALA
PAHALA
PUNALUU
NAALEHU
PONUAPO
KAALUALU
PUU MAHANA
SOUTH POINT
MAUNA LOA TRAIL
AINAPO TRAIL
PUU LOLAU
PUU LEHUA
PUU O UO
PUU ANAHULU
PUU HULUHULU
PUU WAWAA
PUU SHAU
PUU KAWAIWAI
PUU KAWAIHUI
KAWAIHUI STA
HALE POHAKU
HOKUAWEOWEO
KIPUKA PUAULU
MAUNA IKI
KAMAKAIA HILLS
KAPU KAPUKAPU
MAKAALIA
KAHOLENA
PUU ERUPE
KAHUKU PALI
PALI KAHOLO
LAE AUAU
HOOKENA
KONAUNAU
MILOLII
KAPOHOKAMOA
KAPOHOKALOA GULCH
KAHAKAHALULU GULCH
WAILUKU RIVER
HALAI HILL
KEBAU
KAUELE
KAWAIHUI STA
HAKALAU GULCH
HAKALAU
PEPEEKEO POINT
ONOMEA BAY
MAULUA GULCH
KOHALA
KAPAULO
HOKOKAA
WAIPIO VALLEY
WAIMANU VALLEY
KAWAIHAE
KAMAIOLORA
UPOLU POINT
KAGI
POPOO GULCH
CAPE KUMAKAHI
0 5 10 MILES

STATEMENT OF THE PROBLEM

Examination of the recovered samples was undertaken in an effort to resolve the following problems.

1. Changes in major and trace element chemistry with depth might indicate that the well penetrated Mauna Loa Volcano at some depth below Kilauea Volcano, a distinct possibility since Kilauea rests on the flank of Mauna Loa. A lithologic change of this nature could be important as it might effect measurements of physical properties of the rocks or geophysical modeling of the geothermal reservoir. If it could be shown that the recovered rocks are solely Kilauea lavas any changes in chemistry could then be attributed to one or several other causes such as scatter, halmyrolysis, groundwater or hydrothermal alteration, crystal fractionation, or differentiation.

2. Petrographic examination of cores and cutting chips would reveal the mineralogy and petrology of the rocks for correlation with chemical analyses. It might also aid in determining the texture of HGP-A in terms of porosite and permeability. And it would help identify the nature and extent of hydrothermal alteration, requisite for interpreting the chemical data and for defining the hydrothermal system of the well.

3. Secondary mineral assemblages depend on porosite, permeability, chemical composition and degree of crystallinity of host rock, and on the composition and temperature of circulating hydrothermal fluids. Both temperature (Tómasson and Kristmannsdóttir, 1972) and chemical composition of host rock (Ellis, 1967) have been cited as the principal factor in producing a particular assemblage of hydrothermal minerals. Identification of the secondary minerals in HGP-A should provide the

initial reference, as additional geothermal wells are drilled and the data become available, on which factor is dominant in the Hawaiian regime. Knowledge of the hydrothermal minerals would also provide an indication of relatively sealed vs. permeable areas in the well, possibly of composition of the hydrothermal fluid, and particularly of the thermal history and present-day thermal conditions in the well.

GEOLOGIC SETTING

The Hawaiian Islands stretch nearly 2600 km across the North Central Pacific Ocean, decreasing in age from northwest to southeast. The youngest and southeasternmost island of Hawaii is comprised of five volcanoes, two of which, Mauna Loa and Kilauea, constitute the center of present-day volcanic activity in the Hawaiian Islands. Kilauea rests on the flank of Mauna Loa and is, therefore, the younger edifice. Like other Hawaiian shield volcanoes Kilauea has two principal rift zones extending outward from the summit caldera and lying at an obtuse angle to each other. These are the southwest and east rift zones, characterized by open cracks, lines of pit craters, smaller parasitic shields, and spatter cones. Steam vents and warm-water springs and wells are known at several points along the east rift zone (Macdonald, 1973). Eruptions occur at frequent intervals at the summit of Kilauea and along the rift zones. Based on chemistry of summit and east-rift lavas erupted during historic times, Wright and Fiske (1971) believe that "batches" of magma from the shallow reservoir beneath the summit are periodically ejected into the east rift zone and that the more highly differentiated lavas have been held there for periods of more than a century.

I. MAJOR AND TRACE ELEMENT CHEMISTRY

Previous Investigations

Major-element chemistry of Hawaiian lavas has been discussed by many workers (see for example Macdonald and Katsura, 1964; Macdonald, 1968; Wright, 1971; Wright and Fiske, 1971). Most previous analyses have been limited to exposed outcrops of historic and prehistoric flows. Moore (1965) examined 15 fresh basalt samples dredged from the submarine slopes of the east rift zone of Kilauea. Macdonald (1969) discussed the chemistry of very altered basalts cored from Midway Island. Hubbard (1967) reviewed trace-element data on Hawaiian rocks and presented additional analyses of Sr, Rb, Ni, Co, V, and Zr. Gunn (1971) presented new trace-element data in discussing olivine fractionation of Hawaiian basalts. Hart (1973) used trace element analyses of tholeiites dredged from 500 to 5000 m on the east rift of Kilauea to demonstrate the nondependence of trace-element composition on depth of extrusion into sea water.

Materials and Methods

A. Sample Selection. The samples used in this study were taken from the basalt cuttings obtained during drilling of Hawaii Geothermal Project Well-A on the east rift zone of Kilauea Volcano, Hawaii. Nineteen cutting samples from an arbitrarily-chosen interval of approximately 150 m were selected for trace-element analyses on the basis of freshness and high content of chilled marginal glass. Sample depths are listed in Table I. Each bulk samples was hand picked for glass shards assumed to represent the chilled margins of lava flows and, therefore, the most likely representation of the primary magma of that

TABLE I. -- Depth of Sample Below Surface, Plotting Symbol, and Types of Analyses

Depth Below Surface, m	Plotting Symbol	Analyses	
		Major	Trace
0*	O	*	*
186	N	*	*
287	-		*
408	M	*	*
528	L	*	*
650	K	*	*
650A	Ⓚ	*	*
700	-		*
835	J	*	*
900	-		*
976	I	*	*
1106	-		*
1203	H	*	*
1203A	Ⓗ	*	*
1307	G	*	*
1402	F	*	*
1554	E	*	*
1554A	Ⓔ	*	*
1673	D	*	*
1780	C	*	*
1882	B	*	*
1952	A	*	*
1952A	Ⓐ	*	*

Note: Sample O at zero depth is the 1955 Puna flow. Where two samples come from the same depth, the depth followed by the letter "A" represents very altered cutting chips from the same sample bag as the unaltered sample. Plotting symbols for altered samples are circled.

eruption. Where glass was absent or insufficient, dense, dark-gray crystalline rock of flow interiors was hand separated from the bulk sample to provide the freshest possible samples for analyses. In addition, six of the 19 samples were hand picked again for the most altered rock pieces in order to compare and contrast analyses of altered rocks with analyses of the freshest rocks from the same depths in the well. From among these 25 samples, 15 fresh and 4 altered samples were randomly selected and sent to the University of Manitoba for major-element analyses (Table I).

B. Sample Preparation for Trace Element Analyses. Samples were washed in an acid bath followed by 15 minutes of ultrasonic cleaning. They were hand ground at a "clean bench" with an agate mortar and pestle and stored in clean glass vials. Decomposition was achieved in teflon-lined Parr bombs, modified after the method of Buckley and Cranston (1971). Instead of using their recommended quantity of 100 mg of rock powder for each sample, it was found that 200 mg provided a more-easily detectable concentration. Probably 300 mg would have been better still. It was necessary also to modify their recommended use of aqua regia for certain samples. Very altered rocks decomposed readily using their method of wetting the powdered samples with one ml aqua regia, adding six ml concentrated HF, and tightly sealing the bombs, but many samples of fresh rock boiled over repeatedly while heating in the oven. It was found that wetting the rock powder with water instead of aqua regia eliminated this problem. To keep all matrixes the same, one ml aqua regia was added to these samples when diluting to volume. A very few moderately-altered samples failed to decompose satisfactorily by either of the above methods. This

difficulty was resolved by wetting the rock powder with 0.5 ml aqua regia and two drops water. Following dilution to volume the solutions were returned to polypropylene bottles for storage until analysed.

C. Standards. Commercially-prepared standard cation solutions of approximately 1000 µg/ml were used to prepare a combined aqueous standard "A" having the concentration of each element as shown in Table II. These combined quantities represent an upper limit of the concentrations to be expected in samples, based on trace-element concentrations recommended (Flanagan, 1973) for USGS Rock Standard BCR-1, a basalt. Additional standards were prepared daily from combined standard "A". These dilutions were made up individually for each element to bracket the maximum and minimum concentrations expected in the samples based on prior trial analyses. All standards were diluted with a blank solution so that each contained 6% v/v HF, 5.6% w/v H_3BO_3, and 1% v/v aqua regia in order that the standard matrix matched that of the samples after decomposition and dilution.

All reagents used were certified reagent grade chemicals. Distilled and deionized water was used as solvent and dilutant.

TABLE II. -- Recommended Values* for BCR-1 and Elemental Concentrations for Combined Standard "A"

Element	Co	Cr	Cu	Ni	Sr	Rb	Ba	V
BCR-1, ppm	38.0	17.6	18.4	15.8	330.0	46.6	675.0	399.0
Std "A" ug/ml	0.4	0.2	0.2	0.2	4.0	0.4	8.0	4.0

* Flanagan, 1973

D. Analytical Methods. Major element analyses were performed by Kenneth Ramlal at the University of Manitoba. Table III is a summary of the methods used. Precision and accuracy were calculated at the University of Manitoba and are presented in Table IV.

The Graphic Normative Analysis Program developed by Bowen (1971) was used for calculations involving the major-element chemical data including generation of C.I.P.W. norms and various elemental variation diagrams.

Trace element determinations were made on a Perkin-Elmer Atomic Absorption Spectrophotometer, Model 303 for copper and Model 603 for chromium. Intensitron lamps were used for both elements. Except as noted instrumental settings were as recommended by the instrument manufacturer (Perkin-Elmer, 1973).

E. Analytical Results. Precision for Cu and Cr data is shown in Table V. Four samples were selected at random for cursory statistical analyses to see whether the standard deviations were well within the observed changes in concentration. Some types of errors which might account for the observed standard deviations are (1) sample preparation; (2) data-reading errors; and (3) instrumental errors. In view of the accuracy (Table VI) and the greater precision of Cu over Cr for Sample J it is believed that errors due to sample preparation are probably negligible. Data-reading, that is measuring peak heights and calculating concentrations from working curves, must contribute some error, but it is probably uniform and would be difficult to estimate. Background noise was greater and more variable for Cr analyses and more instrumental problems were encountered. This appears to be reflected in the Standard Deviations where generally those for Cr are greater than those

TABLE III. — Summary of Methods used in the Analytical Laboratory, Department of Earth Sciences, University of Manitoba

Element	Method
Si Al Fe (Total) Mg (High) Ca K Ti Mn Zr	X-Ray Fluorescence Spectrometry. Weighted sample plus $Li_2B_4O_7$ plus La_2O_3 heated in a graphite crucible at about 1100°C for a half hour. Resulting glass bead with H_3BO_3 (total weight, 2.1000 grams) ground to -200 mesh and then compressed to 50,000 p.s.i. Elements then simultaneously analyzed on multi-channel ARL X-ray Spectrometer.
Na_2), MgO (Low) and Trace Metals	Atomic Absorption Spectrophotometry. Rock dissolved with HF, H_2SO_4, and HNO_3 in platinum crucibles. Perkin-Elmer 303 A.A.S. used for determinations.
P_2O_5	Colorimetry. Solution as for Na_2O above. The absorption at 430 m of molybdivanadophosphoric acid complex. Unicam sp 500 spectrophotometer.
FeO	Rock decomposed with HF and 1:4 H_2SO_4 solution titrated with $K_2Cr_2O_7$ using Sodium Diphenylamine Sulfonate as indicator.
H_2O^-	Determined by heating sample to constant weight at 110°C.
H_2O (Total)	Determined by heating sample in a stream of dry oxygen in an induction furnace (Temp. 1100°C). H_2O collected on Anhydrone and weighed.
H_2O^+	H_2O (Total) - H_2O^-
S	Determined by heating samples in an induction furnace with oxygen flowing through combustion chamber. SO_2 evolved is then titrated. Leco Induction Furnace and automatic Titrator.
CO_2	Sample decomposed by HCl and heat. CO_2 evolved passed through drying train and collected on Ascarite.
CO_2 (Low S samples)	Determined simultaneously with H_2O (Total). CO_2 collected on Ascarite; small amounts of SO_2 removed on MnO (act).

TABLE IV. — Precision and Accuracy of Major Elements, Department of Earth Sciences, University of Manitoba

Constituent	Concentration %	Instrument Precision, σ	Accuracy of Replicates, σ
SiO_2	59.60	.12	.20
Al_2O_3	9.34	.05	.13
Fe_2O_3 (Total)	10.08	.017	.03
MgO	.404	.04	.10
CaO	10.22	.02	.07
K_2O	2.69	.01	.01
MnO	.41	.01	.01
TiO_2	.48	.02	.02
Na_2O	4.20	.01	.05
H_2O (Total)	1.60	.03	.06
CO_2	1.15	.05	.12
P_2O_5	0.20	.01	.01
FeO	10.92	—	.04
S	0.185	.003	.005

for Cu, indicating that instrumental errors are probably the most significant.

Regression lines were fitted to data points on MgO variation diagrams (Figures 6 through 13) using the program in the manuel of the Hewlett-Packard Model 25 calculator. The equation used in their program is

$$y = a_1 x + a_o$$

$$a_1 = \frac{\Sigma xy - \frac{\Sigma x \Sigma y}{n}}{\Sigma x^2 - \frac{(\Sigma x)^2}{n}}$$

$$a_o = \bar{y} - a_1 \bar{x}$$

where $\bar{y} = \frac{\Sigma y}{n}$ and $\bar{x} = \frac{\Sigma x}{n}$

F. Recommendations. Following are a few recommendations which might aid other investigators using atomic absorption methods to analyze rocks.

(1) Be prepared to spend many hours using and becoming familiar with the instrumentation before attempting to make accurate elemental analyses.

(2) Decompose 200-300 mg of rock powder in 100 ml of solvent. This will increase elemental concentrations but will also increase the amount of dissolved solids in the solution and enhance matrix effects. The use of rock standards should compensate for the matrix effects.

(3) Use whole-rock standards to construct working curves. Synthetic standards are unable to reproduce matrix effects encountered in whole-rock samples. The rock standards should cover a wide range of

TABLE V. -- Precision of Cu and Cr Data

Cr

Sample Depth, m	Sample Symbol	Number of Runs	$\bar{X}$, ppm	Std. Dev., ppm
0	O	5	42.0	± 3.9
835	J	10	225.3	± 12.5
976	I	5	205.3	± 7.8
1554	E	5	131.1	± 8.4

Cu

Sample Depth, m	Sample Symbol	Number of Runs	$\bar{X}$, ppm	Std. Dev., ppm
0	O	4	90.5	± 3.9
835	J	4	120.7	± 1.7
976	I	3	135.6	± 6.9
1554	E	3	107.1	± 2.6

TABLE VI. -- Accuracy of Cu and Cr Data for BCR-1 and AGV-1

	Cu, ppm		Cr, ppm	
BCR-1	17.1 (1)	19.0 (2)	17.2 (1)	16.0 (2)
AGV-1	63.6 (1)	63.0 (2)	12.1 (1)	12.0 (2)

(1) Present report. Claudia Stone, analyst.

(2) Abbey (1973)

concentrations of the elements to be determined.

(4) Check each lamp using the deuterium arc background correction. If baseline drift occurs, the lamp is unstable and probably should not be used.

Results and Discussion

Chemical analyses of lavas from HGP-A are given in Tables VII and VIII and are plotted in Figures 2 through 15. All are quartz-normative tholeiitic basalts and fall well within the tholeiitic field on an alkali:silica diagram (Fig. 2).

In attempting to interpret the chemical data it is necessary to keep in mind that variations in composition could result from one or more of the following processes.

(1) Alteration by groundwater carrying dissolved O_2, H_2CO_2, etc.

(2) Halmyrolysis, the low-temperature interaction between rock and seawater.

(3) Hydrothermal alteration, the interaction between basalt and circulating thermal fluids.

(4) Differentiation of magma from the source region with time, differentiation of "batches" of magma, or crystal fractionation.

(5) Penetration into lavas of another volcanic series.

Groundwater Alteration. Alteration of basalts by groundwater is a distinct possibility for lavas above the zone of sea water saturation and might account for chemical variations observed at shallow depths (Figs. 3 and 4). However, since the amount of island subsidence is unknown, the depth to which groundwater alteration has occurred is

Figure 2. Alkali:silica diagram of HGP-A lavas, Kilauea east rift zone, showing the boundary (solid line) between the tholeiitic and alkalic fields (Macdonald, 1968). Plotting symbols as shown in Table I.

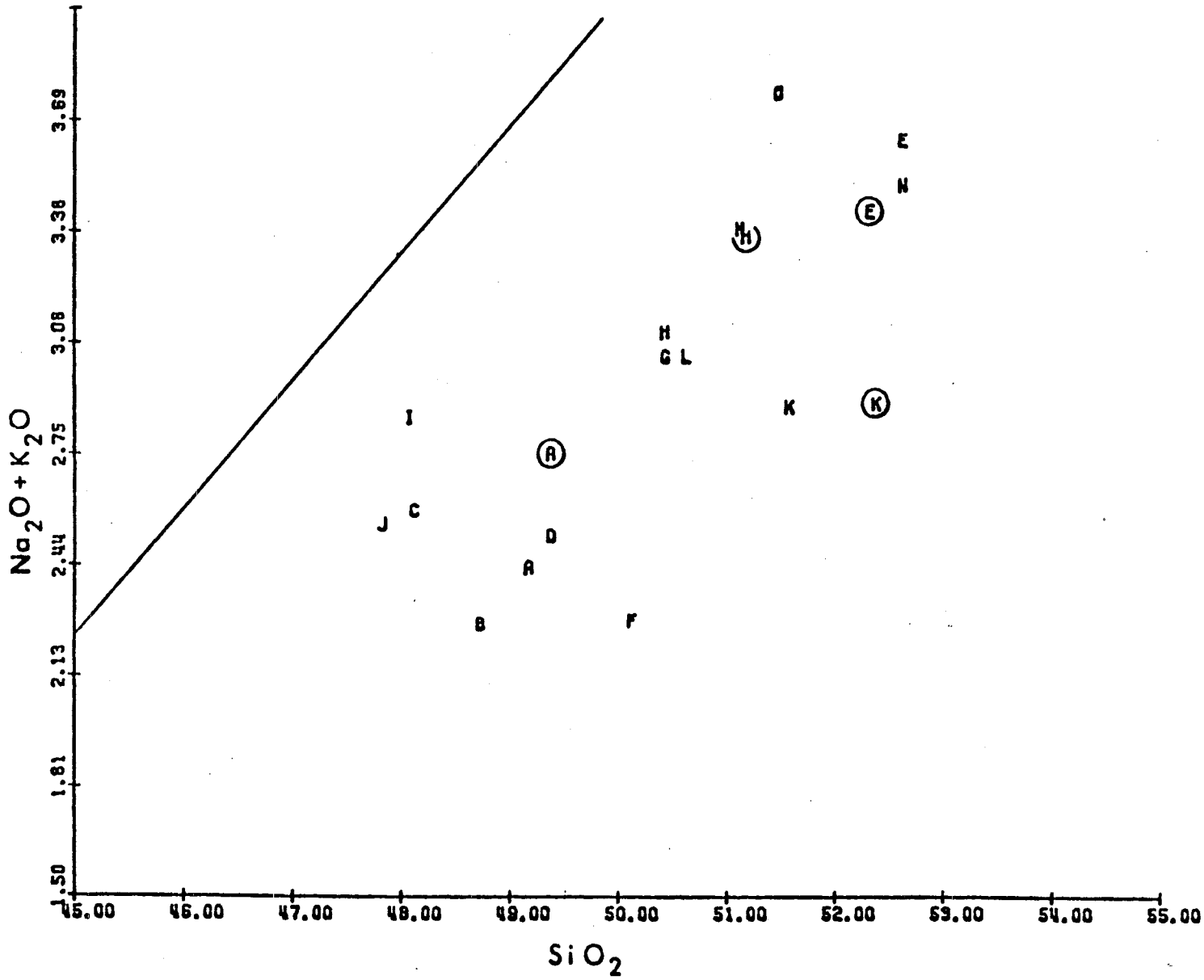
$Na_2O + K_2O$
3.69
3.38
3.08
2.75
2.44
2.13
1.81
1.50
45.00
46.00
47.00
48.00
49.00
50.00
51.00
52.00
53.00
54.00
55.00
SiO_2
O
E
N
E
M
H
H
G L
K
K
I
A
J
C
D
A
B
F

uncertain. The oxide most liable to change due to alteration, MgO, is also the most important for differentiation. It is difficult, therefore, to use chemical data alone to indicate the degree of alteration. Probe analyses or normalizing MgO to Al_2O_3 would aid in these determinations. Even so it appears probable that MgO has been leached by circulating water at shallow depths in the well, and the formation of chlorite has taken up MgO from thermal water permeating the rocks at greater depths.

Halmyrolysis. The action of sea water on pillow basalts dredged from the Mid-Atlantic Ridge has been reviewed by Thompson (1973). His data indicate that Si, Mg, and Ca are the principal elements leached from the basalts and that K and H_2O are the principal ones taken up from sea water. The data suggest that Al, total Fe, and Mn are also leached from the basalt and that P is added. The effects on Na and Ti are less certain, according to Thompson, but more-altered rocks indicate that Na may be leached by extensive weathering. Thompson finds that Cu is taken up by the altered glass rims of pillows but shows little variation in the cyrstalline core. Cr tends to be slightly depleted in the altered portions of pillows but the trends are not consistent. According to Thompson, increasing alteration occurs with increasing distance from the mid-ocean ridge spreading center and thus with increasing age. In studying primary basalts of oceanic layer II, Hart (1973) found that the basalt-sea water interaction results in basalt uptake of K^+, Mg^{2+}, Na^+ and loss of SiO_2, Ca^{2+}, Fe^{2+}, and Mn^{2+}. With increasing H_2O and Fe_2O_3 Hart found a negative correlation for Cr and no correlation for Cu.

If halmyrolysis has occurred to any extent in HGP-A lavas, similar leaching and enrichment trends should be observed, increasing with increasing depth in the well. Although none of the oxides in HGP-A lavas shows a consistent increase or decrease with depth in the well (Table VII and Figures 3 and 4), trends are observed. Of the elements which should be taken up by basalts as a result of halmyrolysis and thus show an increase in weight per cent oxide with depth in the well only MgO, H_2O, and Fe_2O_3 show this trend. K_2O, Na_2O, and P_2O_5 decrease rather than increase. Of the elements shown to be leached by halmyrolysis only the oxides SiO_2 and MnO show a decrease. Al_2O_3 and total Fe remain fairly constant. Cu is leached from very altered samples (Fig. 3, open triantles). The direction of alteration (gain or loss) is not consistent for Cr. An overall increase with depth appears to occur rather than a decrease. Samples K, H, E, and A, with their very altered counterparts show variable uptake and loss trends (Table VII and Figures 3 and 4). Of the elements which should be leached, FeO, MgO, CaO, and MnO show a decrease in most cases, but SiO_2 and Al_2O_3 show increases. Of those which should be taken up by basalts during halmyrolysis H_2O and Na_2O increase but K_2O and P_2O_5 decrease.

It appears that the variations in chemical composition of HGP-A lavas do not correlate satisfactorily with the trends observed by other investigators (Thompson, 1973; and Hart, 1973) for the low-temperature interaction between basalt and sea water. Some of the observations could be accounted for by this process but they appear to be heavily overprinted by another process. This may possibly be due to the relatively young age of the lavas. Some other process, therefore, probably better explains the observed variations in HGP-A lavas.

TABLE VII. -- Chemical Analyses and Norms (C.I.P.W.) of HGP-A Lavas, Kilauea East Rift Zone

Depth, m	0	186	408	528	650
SYMBOL	O	N	M	L	K
SIO2	51.50	52.65	51.15	50.65	51.60
AL2O3	13.07	12.98	13.16	13.32	13.67
FE2O3	2.19	3.16	2.24	2.52	2.44
FEO	10.81	9.29	10.13	9.45	8.76
MGO	4.88	4.97	5.55	6.21	6.15
CAO	8.94	8.78	9.55	10.44	9.72
NA2O	2.88	2.73	2.75	2.52	2.45
K2O	0.89	0.78	0.64	0.51	0.44
H2O	0.12	0.50	0.51	0.71	0.94
CO2		0.03	0.13	0.15	0.14
TIO2	3.79	3.14	3.16	2.72	2.61
P2O5	0.40	0.43	0.35	0.20	0.30
MNO	0.19	0.18	0.18	0.17	0.17
TOTAL	99.66	99.62	99.51	99.57	99.39
Q	5.202	8.775	4.824	3.968	6.751
OR	5.277	4.627	3.801	3.027	2.616
AB	24.453	23.189	23.384	21.416	20.858
AN	20.175	20.939	21.781	23.629	25.156
WO	9.063	8.257	9.453	10.908	8.559
EN	12.195	12.425	13.890	15.533	15.411
FS	12.178	9.635	11.926	11.144	10.138
MT	3.186	4.599	3.254	3.670	3.559
IL	7.223	5.986	6.031	5.188	4.987
AP	0.951	1.022	0.857	0.476	0.715
CC		0.068	0.297	0.343	0.320
TOTAL	99.903	99.523	99.508	99.299	99.072
SALIC	55.108	57.529	53.789	52.039	55.382
FEMIC	44.795	41.993	45.719	47.260	43.690
DI	17.958	16.225	18.638	21.380	16.731
DIWO	9.063	8.257	9.453	10.908	8.559
DIEN	4.451	4.488	4.942	6.098	4.929
DIFS	4.444	3.480	4.243	4.375	3.243
HY	15.478	14.092	16.632	16.204	17.377
HYEN	7.744	7.937	8.949	9.435	10.481
HYFS	7.733	6.155	7.684	6.769	6.896
AL2O3/SIO2	0.254	0.247	0.257	0.263	0.265
FEO/FE2O3	4.936	2.940	4.522	3.750	3.590
D.I.	34.933	36.591	32.019	28.411	30.226

TABLE VII. (Continued) Chemical Analyses and Norms (C.I.P.W.) of HGP-A Lavas from Kilauea East Rift Zone

Depth, m	650A	835	976	1203	1203A
SYMBOL	K	J	I	H	H
SIO2	52.40	47.85	48.10	50.45	51.20
AL2O3	14.21	12.84	13.74	13.19	13.68
FE2O3	3.78	4.05	4.57	4.04	3.88
FEO	7.09	7.41	7.10	7.57	7.18
MGO	4.25	8.35	7.85	6.41	5.83
CAO	8.36	9.76	9.43	9.52	9.34
NA2O	2.59	1.88	2.44	2.48	2.55
K2O	0.31	0.68	0.42	0.62	0.82
H2O	1.48	2.52	1.70	1.18	1.14
CO2	0.28	0.42	0.44	0.32	0.32
TIO2	3.12	2.52	2.80	2.64	2.76
P2O5	0.27	0.23	0.26	0.30	0.29
MNO	0.12	0.20	0.20	0.18	0.16
TOTAL	98.26	98.71	99.05	98.90	99.15
Q	13.935	4.103	3.754	6.883	7.774
OR	1.864	4.071	2.506	3.704	4.887
AB	22.304	15.116	20.945	21.218	21.762
AN	26.696	24.909	25.540	23.283	23.660
WO	4.975	8.322	7.168	8.536	7.984
EN	10.772	21.068	19.738	16.142	14.644
FS	5.056	6.556	5.059	6.611	5.768
MT	5.578	5.949	6.690	5.923	5.674
IL	6.030	4.849	5.369	5.070	5.287
AP	0.651	0.552	0.622	0.718	0.693
CC	0.648	0.968	1.010	0.736	0.734
TOTAL	98.509	97.462	98.300	98.825	98.867
SALIC	64.799	49.199	52.644	55.089	58.083
FEMIC	33.710	48.263	45.655	43.736	40.784
DI	9.631	15.947	13.681	16.464	15.384
DIWO	4.975	8.322	7.168	8.536	7.984
DIEN	3.168	5.815	5.184	5.624	5.309
DIFS	1.487	1.810	1.329	2.304	2.091
HY	11.173	19.999	18.284	14.825	13.012
HYEN	7.604	15.252	14.554	10.517	9.335
HYFS	3.569	4.747	3.730	4.308	3.677
AL2O3/SIO2	0.271	0.268	0.286	0.261	0.267
FEO/FE2O3	1.876	1.830	1.554	1.874	1.851
C.I.	38.103	24.289	27.104	31.806	34.423

TABLE VII. (Continued) Chemical Analyses and Norms (C.I.P.W.) of HGP-A Lavas from Kilauea East Rift Zone

Depth, m	1307	1402	1554	1554A	1673
SYMBOL	G	F	E	E	D
SIO2	50.45	50.15	52.65	52.35	49.40
AL2O3	13.39	13.30	13.47	13.41	13.54
FE2O3	4.00	3.11	4.04	4.20	3.58
FEO	7.38	8.25	7.29	6.61	7.42
MGO	6.77	7.51	4.93	5.46	7.68
CAO	9.43	10.46	8.40	8.32	9.83
NA2O	2.49	2.09	2.80	2.71	2.25
K2O	0.54	0.20	0.84	0.73	0.28
H2O	1.19	1.09	1.08	1.28	1.32
CO2	0.36	0.27	0.32	0.28	0.35
TIO2	2.76	2.48	2.62	2.64	2.62
P2O5	0.31	0.24	0.42	0.38	0.29
MNO	0.17	0.17	0.17	0.16	0.17
TOTAL	99.24	99.32	99.03	98.53	98.73
Q	6.819	5.882	10.494	10.912	5.568
OR	3.215	1.190	5.012	4.378	1.676
AB	21.231	17.806	23.925	23.273	19.284
AN	23.946	26.498	21.917	22.602	26.353
WO	7.875	9.375	6.409	6.252	7.884
EN	16.990	18.832	12.399	13.801	19.373
FS	6.052	8.861	6.098	4.675	6.743
MT	5.844	4.540	5.915	6.180	5.257
IL	5.282	4.742	5.025	5.089	5.040
AP	0.740	0.572	1.005	0.913	0.696
CC	0.825	0.618	0.735	0.646	0.806
TOTAL	98.819	98.917	98.933	98.723	98.680
SALIC	55.211	51.376	61.349	61.166	52.881
FEMIC	43.608	47.541	37.585	37.557	45.799
DI	15.137	18.148	12.422	12.003	15.145
DIWO	7.875	9.375	6.409	6.252	7.884
DIEN	5.355	5.966	4.031	4.296	5.387
DIFS	1.907	2.807	1.982	1.455	1.875
HY	15.780	18.920	12.483	12.725	18.855
HYEN	11.635	12.866	8.368	9.505	13.987
HYFS	4.145	6.054	4.116	3.220	4.868
AL2O3/SIO2	0.265	0.265	0.256	0.256	0.274
FEO/FE2O3	1.845	2.653	1.804	1.574	2.073
D.I.	31.265	24.878	39.431	38.564	26.528

TABLE VII. (Continued) Chemical Analyses and Norms (C.I.P.W.) of HGP-A Lavas from Kilauea East Rift Zone

Depth, m	1780	1882	1952	1952A
SYMBOL	C	B	A	(A)
SIO2	48.15	48.75	49.20	49.40
AL2O3	13.48	13.43	13.18	12.94
FE2O3	4.97	3.82	2.78	3.48
FEO	7.43	7.37	8.81	7.26
MGO	7.61	7.71	9.08	8.36
CAO	9.72	10.44	9.65	9.77
NA2O	2.48	2.12	2.18	2.66
K2O	0.12	0.16	0.26	0.10
H2O	1.36	2.00	1.04	2.30
CO2	0.39	0.30	0.18	0.16
TIO2	2.70	2.46	2.36	2.48
P2O5	0.24	0.24	0.22	0.15
MNO	0.17	0.17	0.17	0.15
TOTAL	98.82	98.97	99.11	99.21
Q	4.513	5.153	2.047	3.064
OR	0.718	0.955	1.550	0.596
AB	21.236	18.126	18.612	22.687
AN	25.597	26.934	25.638	23.256
WO	7.983	9.143	8.379	9.850
EN	19.179	19.402	22.817	20.986
FS	5.460	6.701	10.393	6.693
MT	7.292	5.596	4.067	5.086
IL	5.189	4.721	4.522	4.748
AP	0.575	0.574	0.526	0.358
CC	0.898	0.689	0.413	0.367
TOTAL	98.638	97.994	98.964	97.691
SALIC	52.063	51.167	47.847	49.603
FEMIC	46.576	46.826	51.117	48.088
DI	15.268	17.562	16.206	13.886
DIWO	7.983	9.143	8.379	9.850
DIEN	5.671	6.258	5.378	6.851
DIFS	1.614	2.161	2.449	2.185
HY	17.354	17.684	25.383	18.644
HYEN	13.508	13.144	17.439	14.136
HYFS	3.846	4.540	7.943	4.508
AL2O3/SIO2	0.280	0.275	0.268	0.262
FEO/FE2O3	1.495	1.929	3.169	2.086
D.I.	26.466	24.234	22.210	26.347

Figure 3. Changes in concentrations of Cu and Cr with depth in HGP Well-A lavas, Kilauea east rift zone. Plotting symbols as shown in Table I. Open squares represent additional data points; open triangles represent very altered samples from the same depth as the unaltered one.

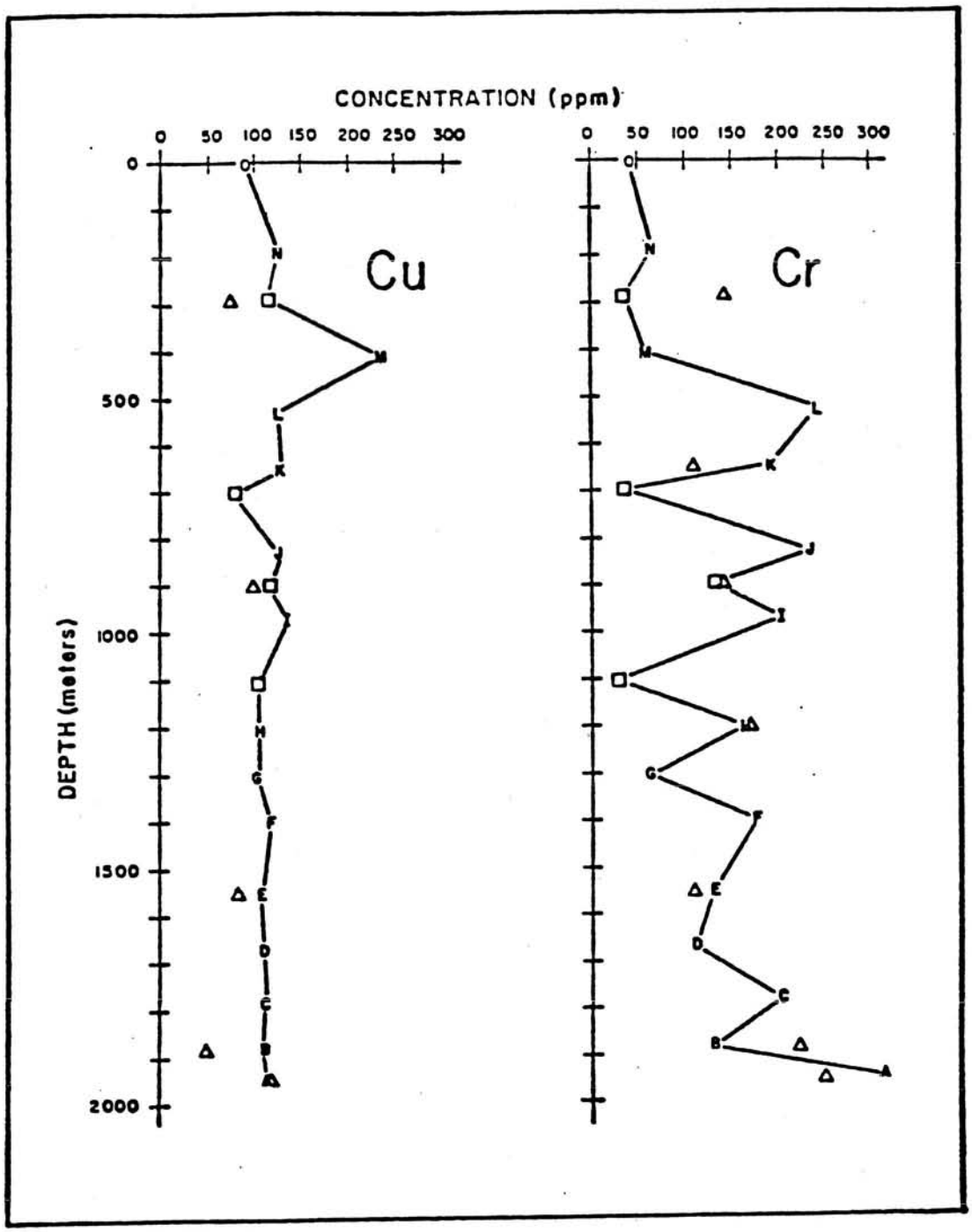
CONCENTRATION (ppm)
0 50 100 150 200 250 300
Cu
Cr
DEPTH (meters)
0
500
1000
1500
2000

Figure 4. Depth vs. oxides of HGP-A lavas, Kilauea east rift zone. Plotting symbols as shown in Table I.

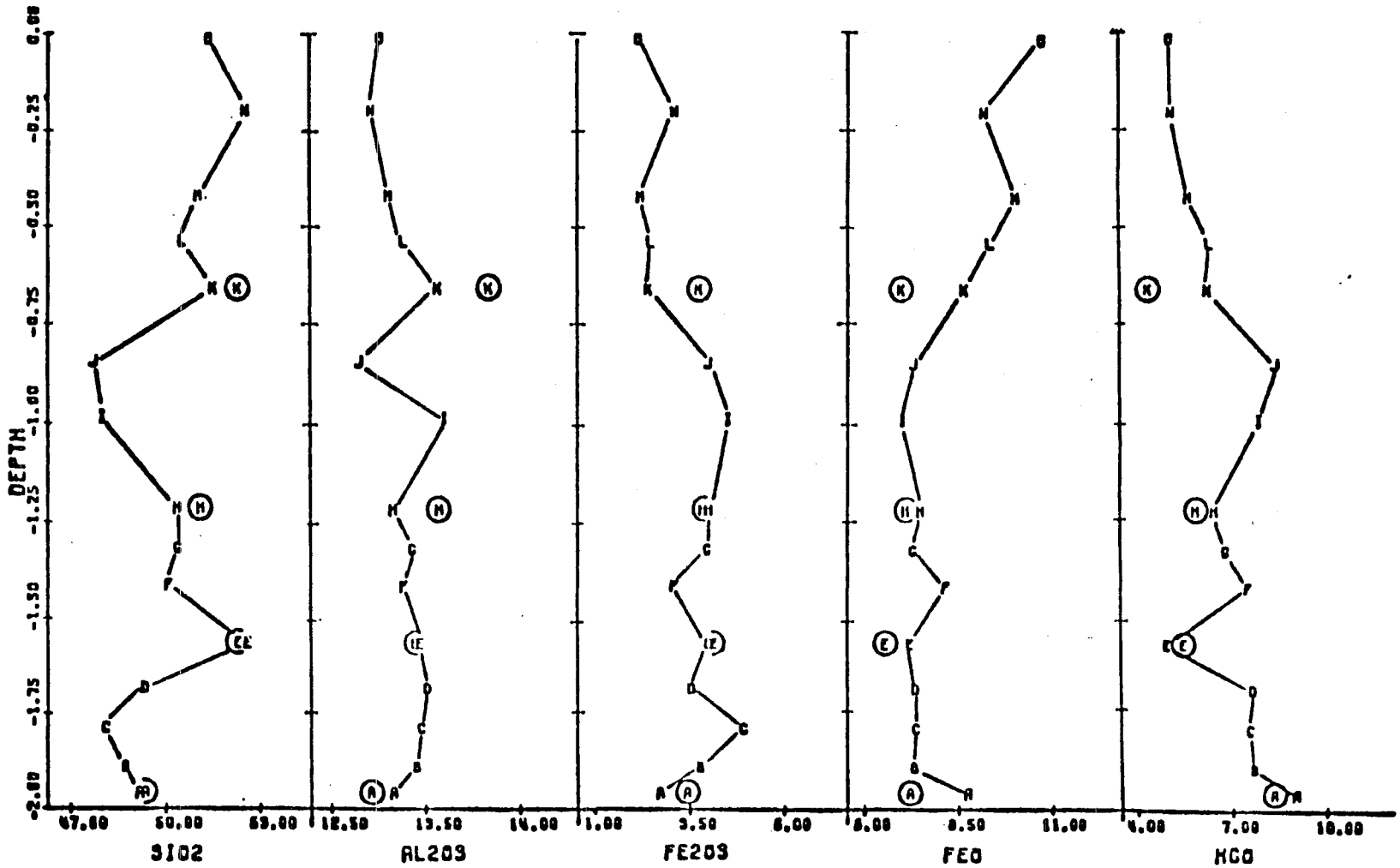
DEPTH
0.00
-0.25
-0.50
-0.75
-1.00
-1.25
-1.50
-1.75
-2.00
47.00
50.00
53.00
SIO2
12.50
13.50
14.00
AL2O3
1.00
3.50
6.00
FE2O3
8.00
8.50
11.00
FEO
6.00
7.00
10.00
MGO

(A) (B) (C) (D) (E)

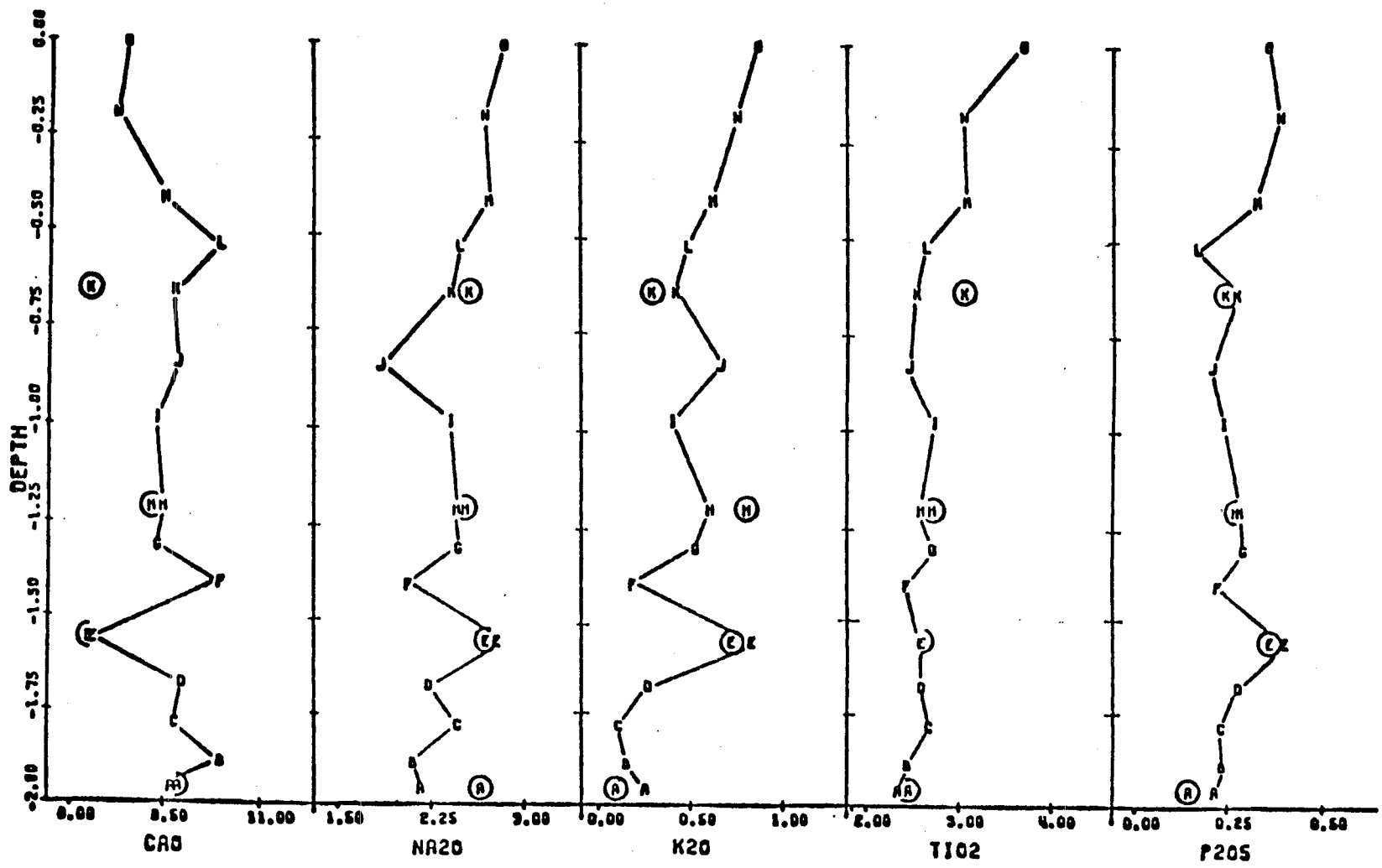
DEPTH
0.00
-0.25
-0.50
-0.75
-1.00
-1.25
-1.50
-1.75
-2.00
0.00
5.50
11.00
CAO
1.50
2.25
3.00
NA2O
0.00
0.50
1.00
K2O
2.00
3.00
4.00
TIO2
0.00
0.25
0.50
P2O5

(F) (G) (H) (I) (J)

Hydrothermal Alteration. The effects of hydrothermal alteration on the chemical composition of basalts from high-temperature geothermal fields in Iceland have been reviewed by Kristmannsdóttir (1975). She stated that systematic changes in chemistry with depth are not observed in Icelandic basalts and that the major changes found in the altered rocks are hydration and oxidation, with some enrichment of SiO_2 in a few samples. She concluded, "The sharp changes in mineralogy of the rocks are thus not reflected by marked changes in chemistry" (p. 442). While sharp changes may not be apparent in HGP-A lavas, it seems probable that leaching and enrichment in certain oxides have occurred even though they would be difficult to estimate beyond what is seen in samples A, E, H, and K and their altered counterparts (Fig. 4). The variable trends (gain and loss) noted for certain oxides may be due to variable permeability and/or temperature of water at different depths in the well.

Differentiation and Crystal Fractionation. Wright (1971) and Wright and Fiske (1971) studied the summit and rift-zone lavas of Kilauea. They concluded that summit lavas are undifferentiated, which they defined as lavas with MgO greater than 6.8 per cent and which are chemically related to one another by the addition or subtraction of magnesian olivine, termed 'olivine control.' They also concluded that differences in chemical composition are due in part to secular variations in composition of magma from the source region. Wright and Fiske (1971) claimed that rift-zone lavas can be segregated into three distinct groups. (1) Undifferentiated lavas similar in composition to summit lavas. (2) Differentiated lavas with MgO lower than 6.8 per

cent, whose chemical composition is due to removal of minerals in addition to olivine, primarily clinopyroxene and feldspar. (3) Hybrid lavas produced by mixing of summit magmas with differentiated magmas in varying proportions and, therefore, containing MgO in any amount. Wright and Fiske (1971) derived the hybrid lavas by computer modeling, working with summit and rift lavas of known compositions and with eruptions of geologically short duration. On the basis of their investigations the authors suggested that differentiated and hybrid lavas appear to form "a greater proportion of the younger Kilauea lava flows than they do of the older prehistoric flows"(p. 14).

A correlation of HGP-A lavas with deeply buried summit lavas would possibly enable similar conclusions to be made with respect to origin of HGP-A magmas. Such data do not exist for summit lavas, however, so that it is possible only to discuss major trends of differentiation.

Based on a plot of MgO against depth (Fig. 4-E), three zones are apparent in the HGP-A stratigraphic sequence. (1) From 1952 m to 1673 m the lavas appear to be undifferentiated, with MgO greater than 6.8 per cent but decreasing upwards in the well from 9.08 to 7.68 per cent (samples A - D). (2) Between 1554 m and 835 m the MgO content is both greater and less than 6.8 per cent (samples E - K). (3) Above 650 m the lavas appear to be differentiated, with MgO less than 6.8 per cent, and again decreasing upwards from 6.15 to a low of 4.88 per cent (samples J - O). Sample O is from the 1955 Puna flow, about which Wright and Fiske (1971) stated that, "The earliest lavas erupted were the most differentiated (MgO $\sim$ 5 per cent) that had been observed in Kilauean eruptions up to that time" (p. 21).

In the AFM diagram (Fig. 5) HGP-A lavas plot on the variation trend

Figure 5. AFM diagram of HGP-A lavas, Kilauea east rift zone. Plotting symbols as shown in Table I. Solid line represents variation trend line for Kilauea; O represents olivine composition (Macdonald and Katsura, 1964). CPX represents augite composition (Core 2, this report). OPX represents hypersthene composition (Wright, 1971). In AFM diagram, $A = Na_2O + K_2O$, $F = FeO + .89981 * Fe_2O_3 + MnO$, and $M = MgO$.

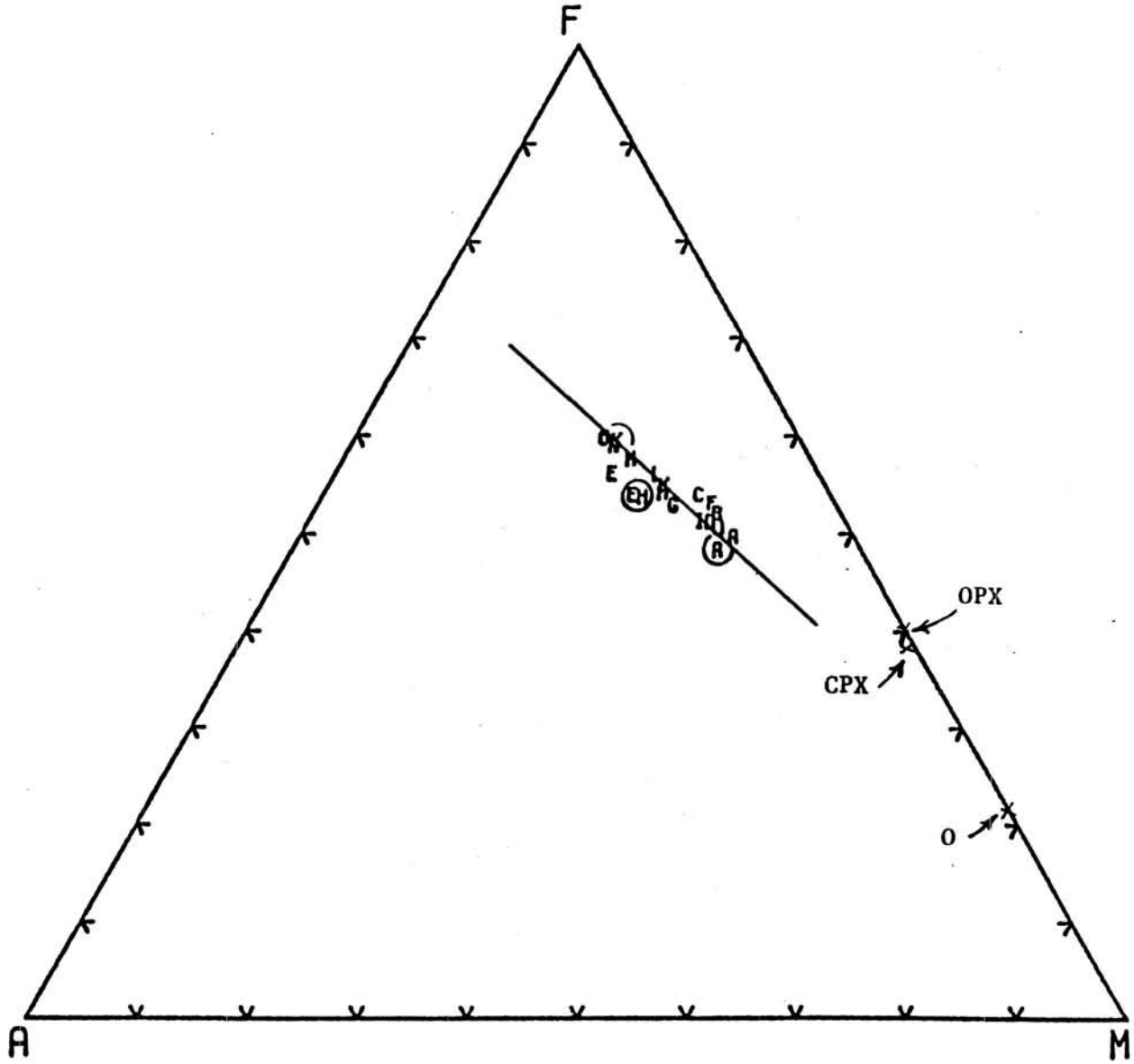
F
A
M
OPX
CPX
O

line of Kilauea tholeiitic rocks (Macdonald and Katsura, 1964) and are seen to trend from more to less magnesia rich. However, whether they are controlled by olivine or orthopyroxene cannot be distinguished.

In all MgO variation diagrams, Figures 6 through 13, the slopes of all regression lines are negative to nearly flat except Figure 9, CaO. The negative slope found for SiO_2, Na_2O, and K_2O is the expected trend if magma from the source region is becoming more differentiated with time. Figure 9 is a plot of MgO against CaO. CaO is a good indicator of olivine vs. clinopyroxene and feldspar crystallization as CaO increases with decreasing MgO during crystallization of olivine, and it decreases with decreasing MgO during crystallization of clinopyroxene and feldspar. This plot (Fig. 9) shows considerable scatter; but the overall trend indicates that removal of clinopyroxene and feldspar may dominate differentiation at the source region.

Figure 14 is a simplified plot of FeO + MgO against FeO/MgO (Macdonald and Katsura, 1964) indicating that early HGP-A lavas may fall on the trend of olivine-controlled differentiates. But beginning at a depth of 1307 m (symbol G), and excluding the interval from 976 m to 835 m (symbols I and J), there is a distinct horizontal trend corresponding to the right-hand limb of Macdonald and Katsura's Figure 4, indicating possible control of these later lavas by separation of clinopyroxene and feldspar.

Trace-element concentrations are presented in Table VIII and are plotted against depth in the well in Figure 3. Hart (1973) has shown that trace-element composition is not related to extrusion of basaltic lavas into sea water at depth. The effects of halmyrolysis, groundwater and hydrothermal alteration, discussed above, appear to be

Figure 6. Plot of MgO against SiO_2, HGP-A lavas, Kilauea east rift zone. Plotting symbols as shown in Table I.

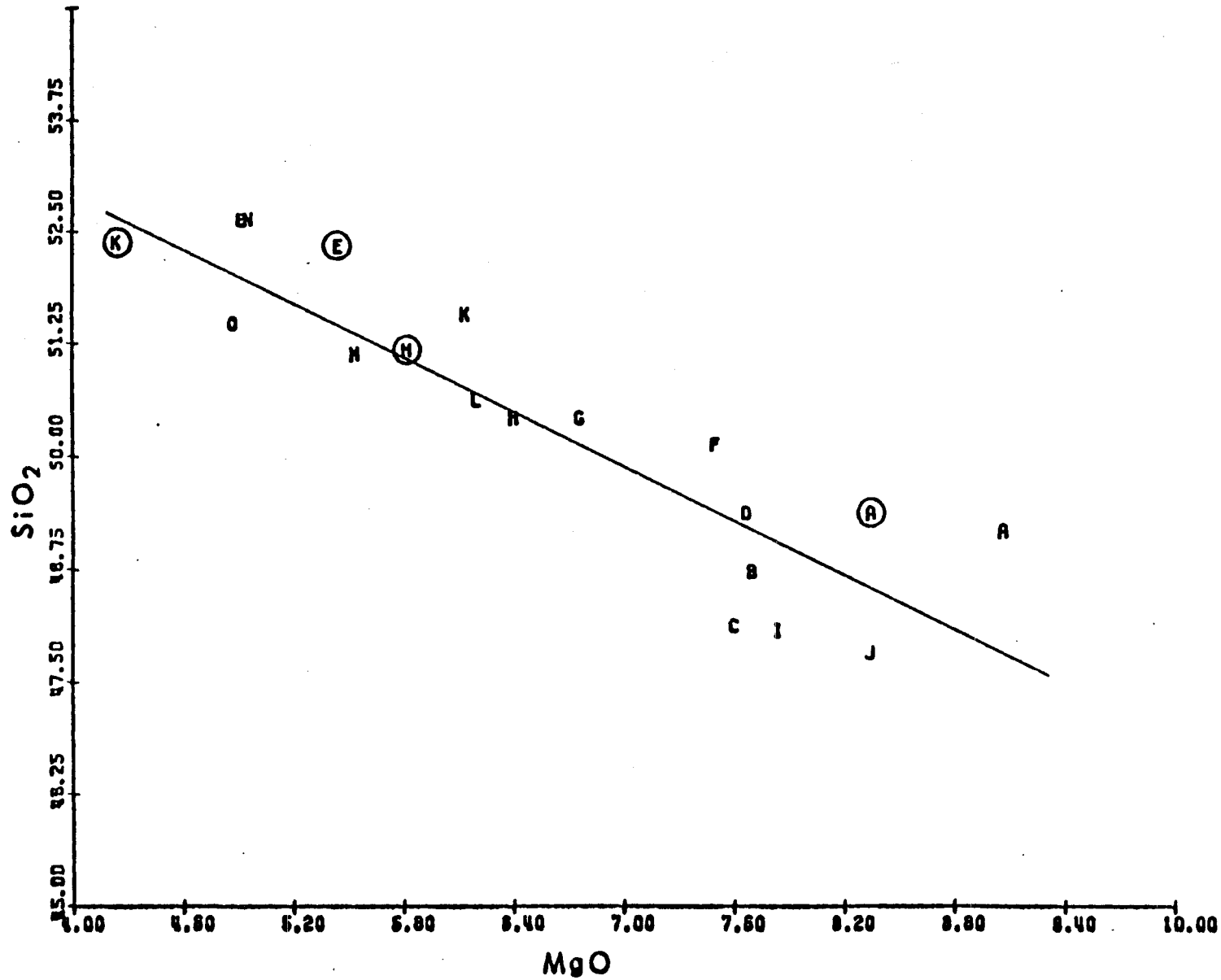
SiO2
MgO
53.75
52.50
51.25
50.00
48.75
47.50
46.25
45.00
4.00
4.80
5.20
5.80
6.40
7.00
7.60
8.20
8.80
9.40
10.00
K
EN
E
O
K
N
H
L
M
G
F
D
A
A
B
C
I
J

Figure 7. Plot of MgO against Al_2O_3, HGP-A lavas, Kilauea east rift zone. Plotting symbols as shown in Table I.

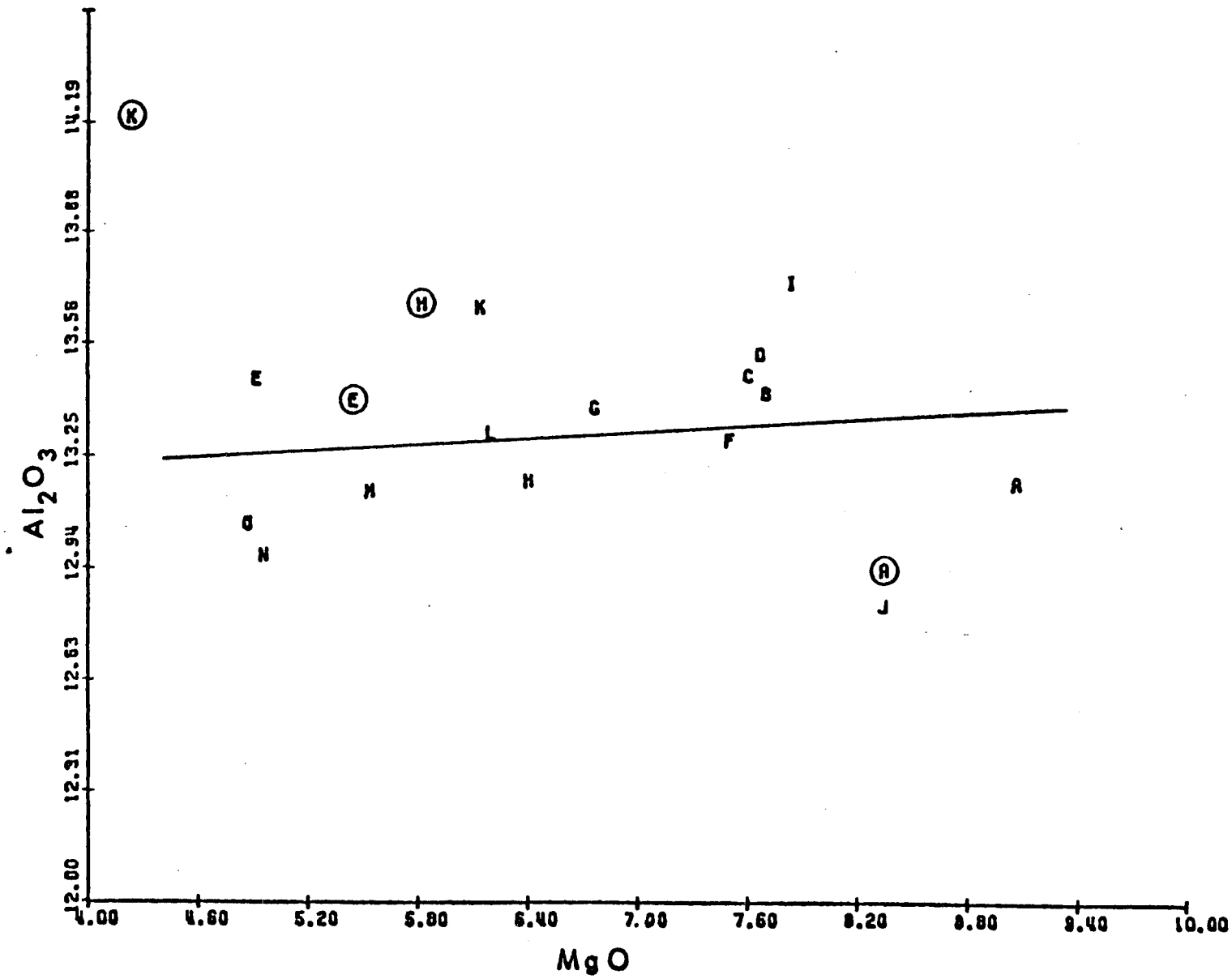
14.19
13.88
13.58
13.25
12.94
12.63
12.31
12.00
Al_2O_3
4.00
4.60
5.20
5.80
6.40
7.00
7.60
8.20
8.80
9.40
10.00
MgO
K
H
K
I
D
C
B
E
E
G
L
F
M
H
A
G
N
A
J

Figure 8. Plot of MgO against Total FeO, HGP-A lavas, Kilauea east rift zone. Plotting symbols as shown in Table I.

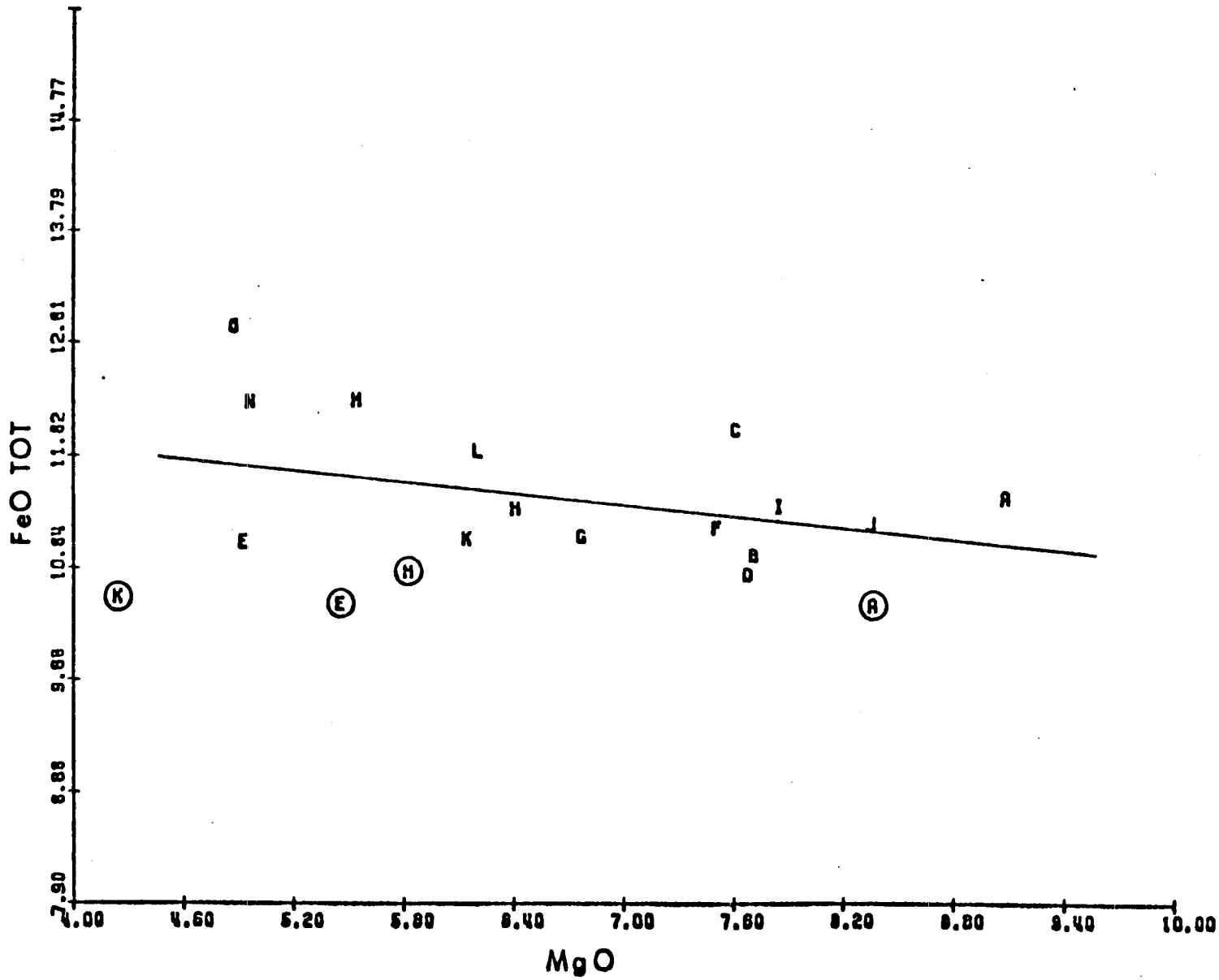
FeO TOT
14.77
13.79
12.81
11.82
10.84
9.88
8.88
7.90
4.00
4.60
5.20
5.80
6.40
7.00
7.60
8.20
8.80
9.40
10.00
MgO
G
N
M
L
C
H
I
A
E
K
G
F
J
B
D
K
E
M
A

Figure 9. Plot of MgO against CaO, HGP-A lavas, Kilauea east rift zone. Plotting symbols as shown in Table I.

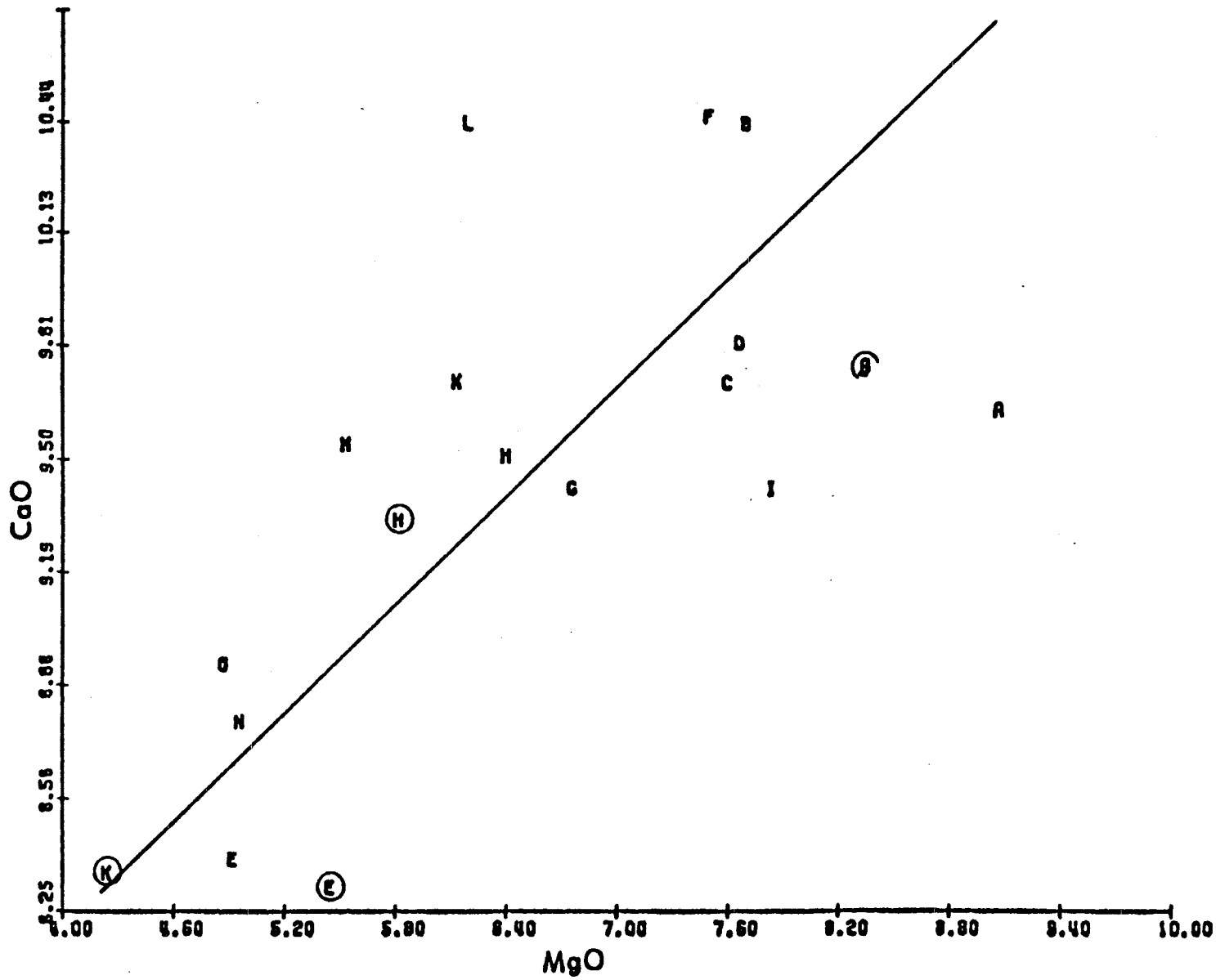
CaO
MgO
10.44
10.13
9.81
9.50
9.19
8.88
8.56
8.25
4.00
4.60
5.20
5.80
6.40
7.00
7.60
8.20
8.80
9.40
10.00
L
F
B
D
C
A
K
M
H
G
I
O
N
E

Figure 10. Plot of MgO against K_2O, HGP-A lavas, Kilauea east rift zone. Plotting symbols as shown in Table I.

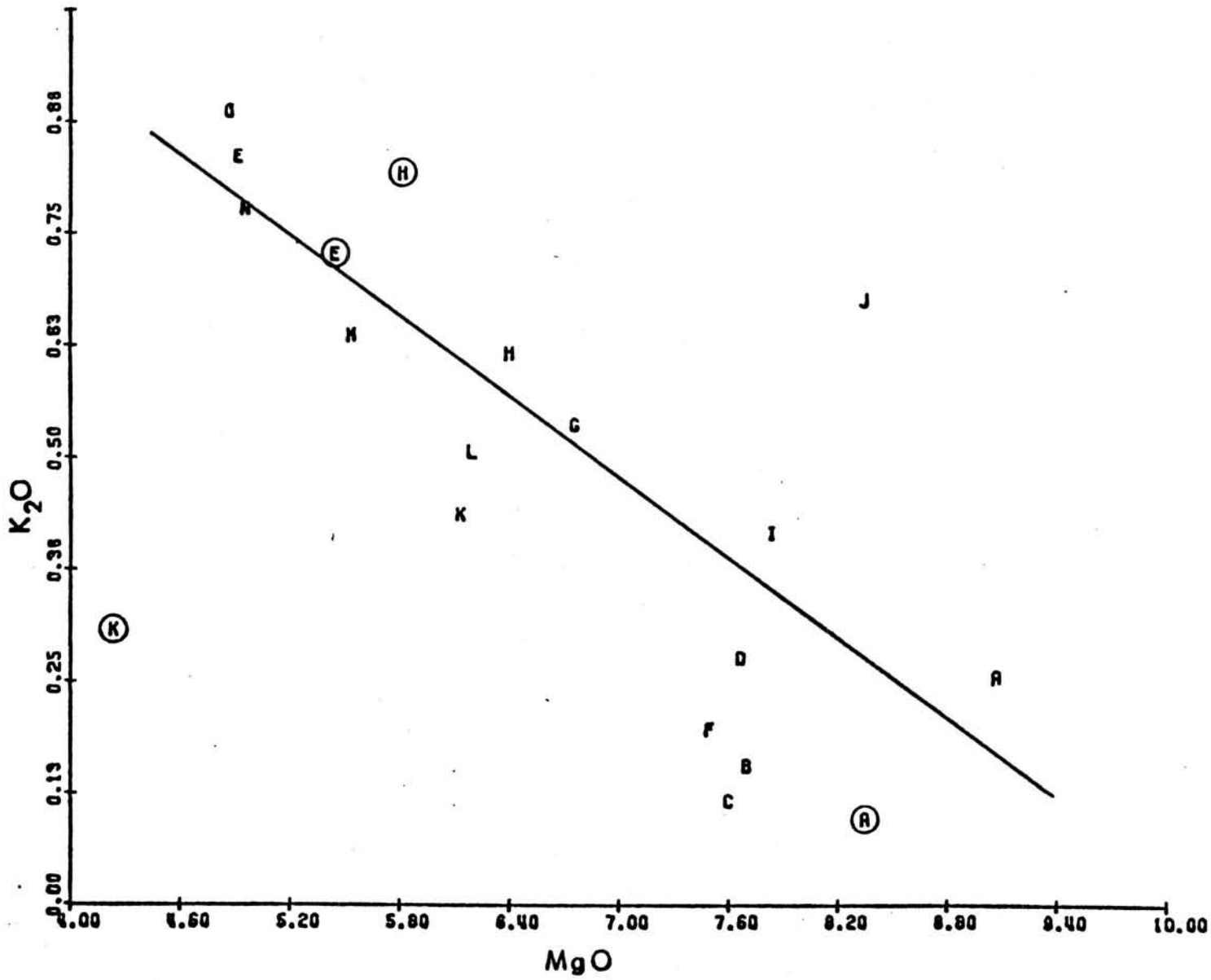
K2O
MgO
0.00
0.13
0.25
0.38
0.50
0.63
0.75
0.88
4.00
4.60
5.20
5.80
6.40
7.00
7.60
8.20
8.80
9.40
10.00
G
E
N
H
E
N
H
G
L
K
K
J
I
D
A
F
B
C
A

Figure 11. Plot of MgO against Na_2O, HGP-A lavas, Kilauea east rift zone. Plotting symbols as shown in Table I.

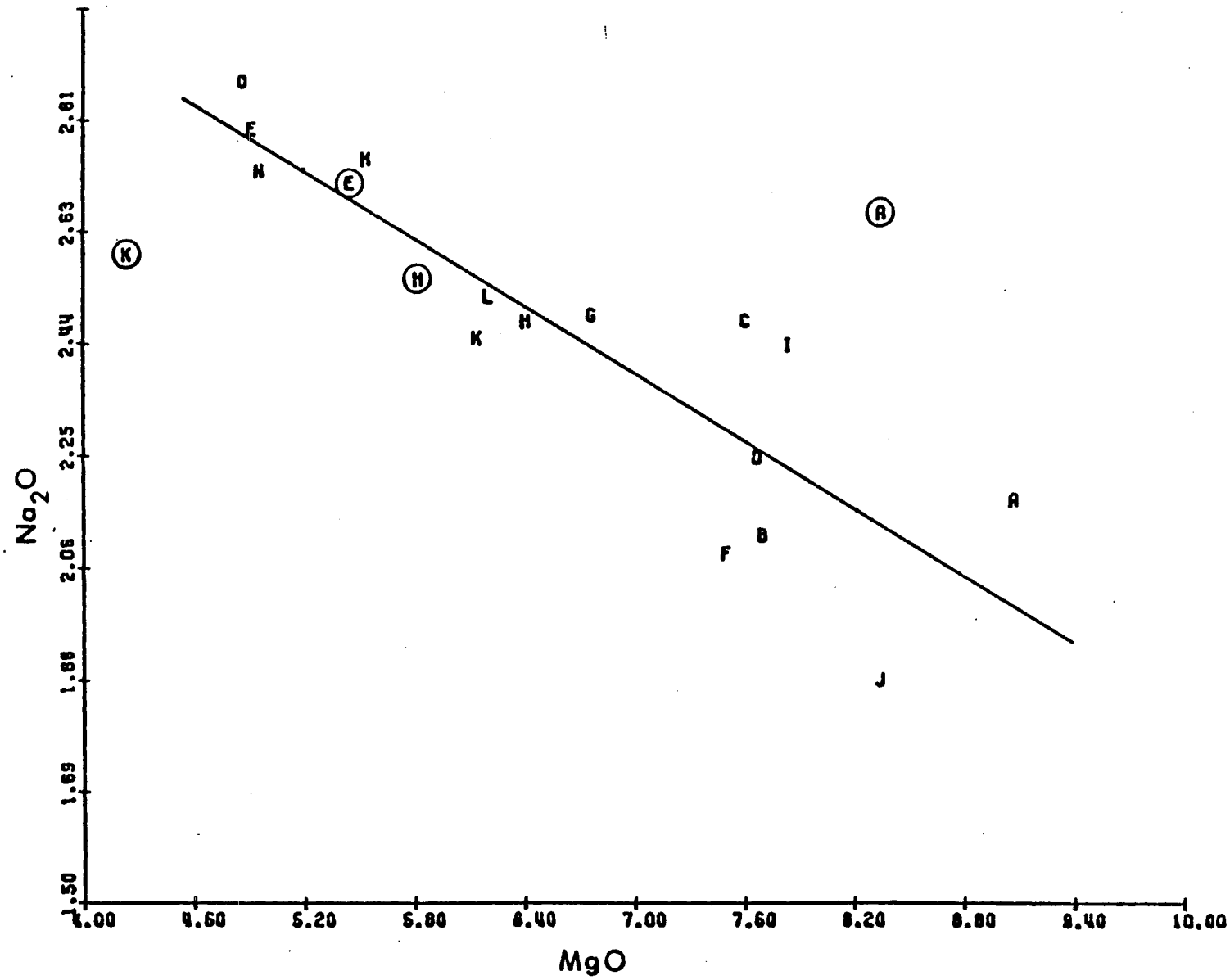
Na2O
MgO
2.81
2.63
2.44
2.25
2.06
1.88
1.69
1.50
4.00
4.60
5.20
5.80
6.40
7.00
7.60
8.20
8.80
9.40
10.00
O
E
N
K
E
K
H
L
K
H
G
C
I
D
A
B
F
J
A

Figure 12. Plot of MgO against TiO_2, HGP-A lavas, Kilauea east rift zone. Plotting symbols as shown in Table I.

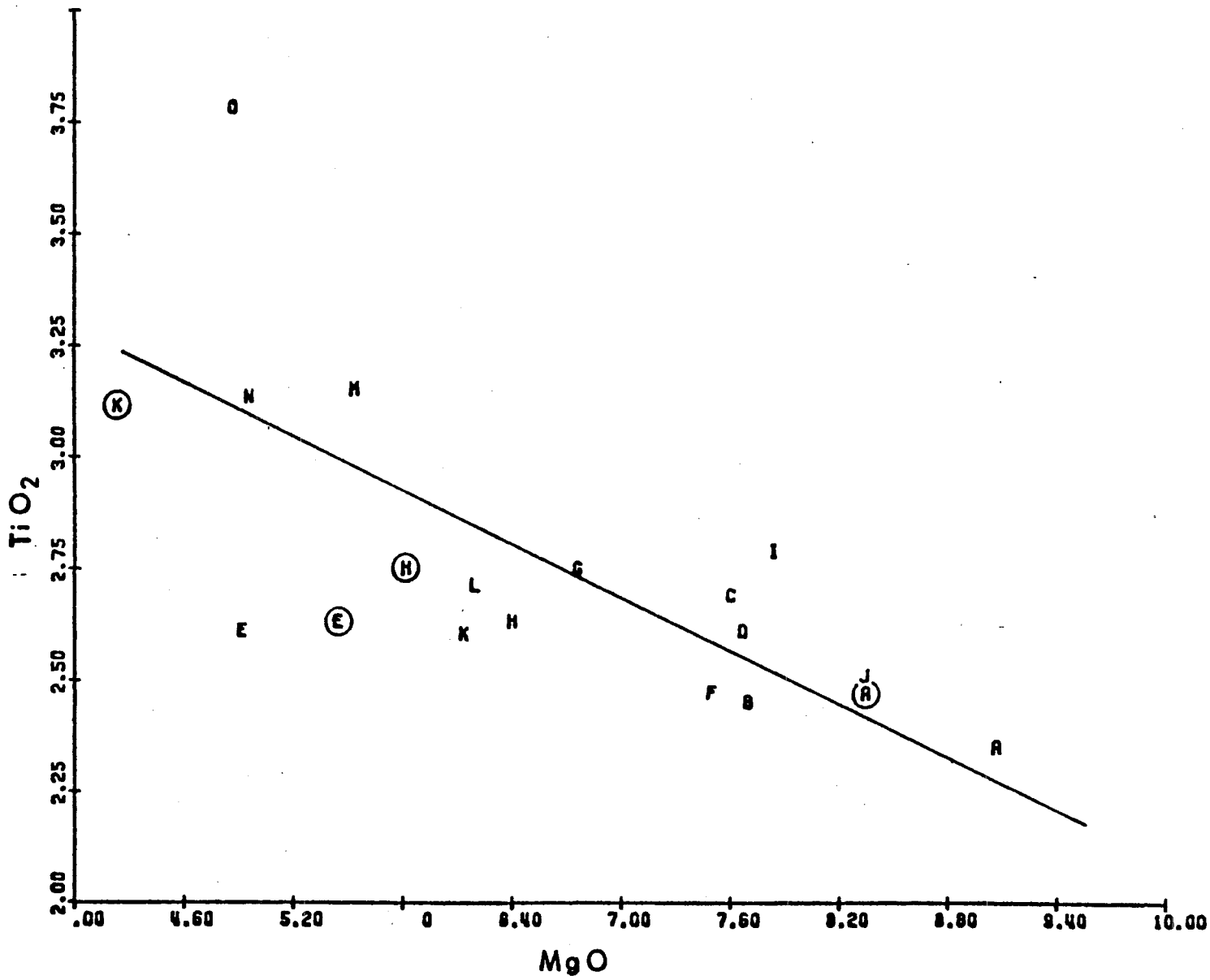
TiO2
MgO
3.75
3.50
3.25
3.00
2.75
2.50
2.25
2.00
.00
4.60
5.20
0
6.40
7.00
7.60
8.20
8.80
9.40
10.00
O
K
N
M
H
L
G
I
C
E
E
K
H
D
J
A
F
B
A

Figure 13. Plot of MgO against P_2O_5, HGP-A lavas, Kilauea east rift zone. Plotting symbols as shown in Table I.

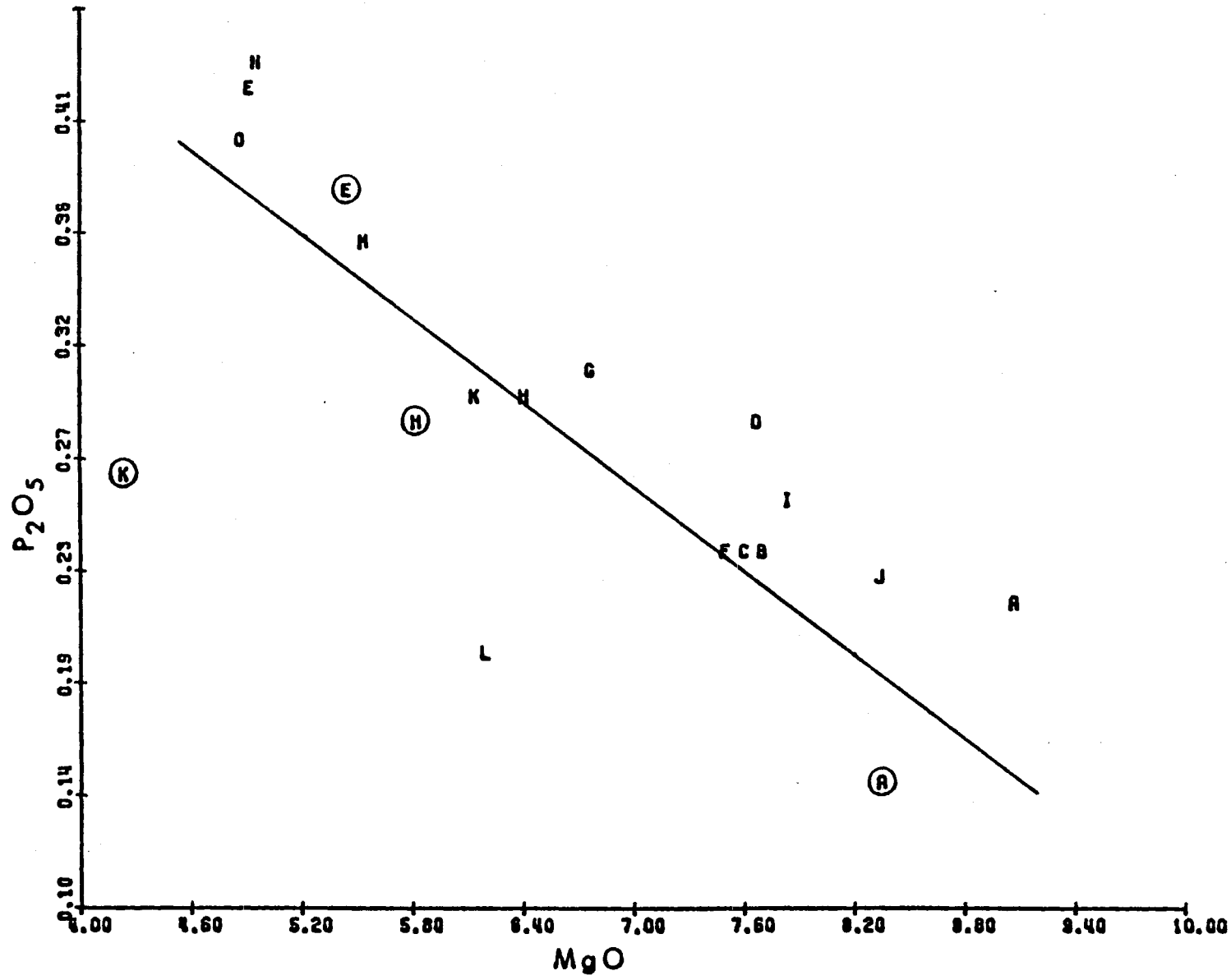
P2O5
0.10
0.14
0.19
0.23
0.27
0.32
0.36
0.41
MgO
4.00
4.60
5.20
5.80
6.40
7.00
7.60
8.20
8.80
9.40
10.00
N
E
O
E
M
G
K
H
H
D
K
I
F C B
J
A
L
A

Figure 14. Plot of FeO Total/MgO against FeO Total + MgO, HGP-A lavas, Kilauea east rift zone. Plotting symbols as shown in Table I.

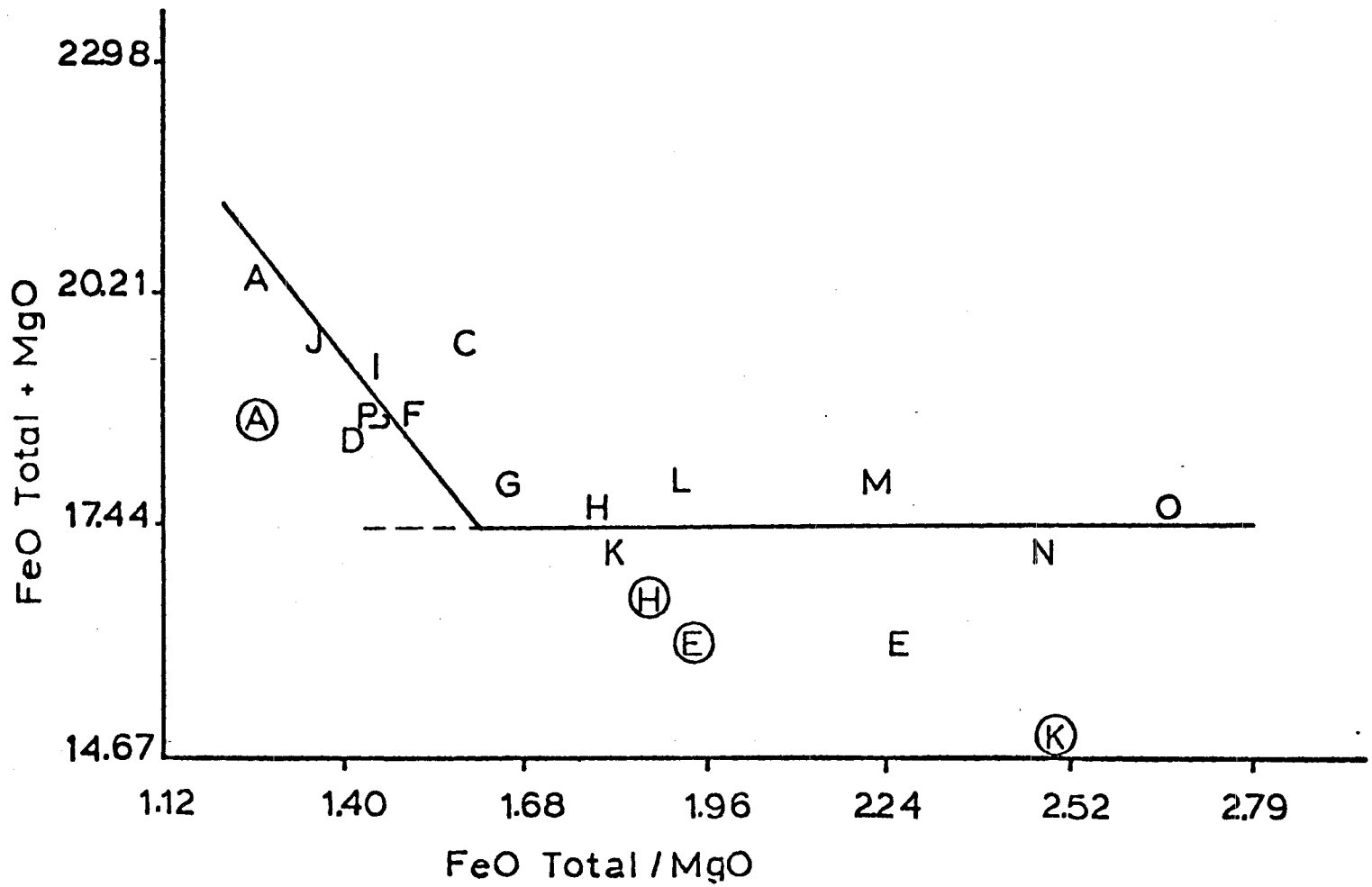
22.98
20.21
17.44
14.67
FeO Total + MgO
1.12
1.40
1.68
1.96
2.24
2.52
2.79
FeO Total / MgO
A
J
I
C
P
F
D
G
H
L
M
O
K
N
E
A
H
E
K

variable so that observed trends may be related to crystal fractionation or differentiation.

Chromium concentrations vary considerably with depth (Fig. 3) and exhibit a great deal of scatter when plotted against MgO (Fig. 15). However, the trend appears to be covariant with MgO. Chromium is not taken up by olivine except where it has inclusions of chromite, chrome spinel, or chrome diopside (Turekian, 1963). Inclusions, however, are not observed in olivine phenocrysts under the microscope. Chromium is removed early in the pyroxene during fractional crystallization and diminishes with progressive crystallization. The observed scatter might represent crystallization of "batches" of magma, with the injection of each new batch again increasing the concentration.

Below 1000 m Cu is nearly uniform in concentration which may be the result of homogenizing due to alteration (E. Cray, personal communication, 1977), or it might be that the source region is homogeneous with respect to Cu which seems less likely because other elements seem to indicate that differentiation may be occurring. Above 1000 m the variation in Cu concentration is still small except for the sample at 408 m (symbol M, Fig. 3) which appears to be "normal" with respect to other oxides. Since the very altered samples, represented by open triangles in Figure 3, show that Cu is leached from HGP-A basalts during alteration, the high concentration of Cu in sample may be an unaltered depth interval or at least a less-intensely altered zone. It might also represent a zone of Cu deposition as a result of subaerial weathering, greater permeability, or variable temperature.

Penetration into Lavas of Another Volcanic Series. Another

Figure 15. Plot of MgO against Cr, HGP-A lavas, Kilauea east rift zone. Plotting symbols as shown in Table I.

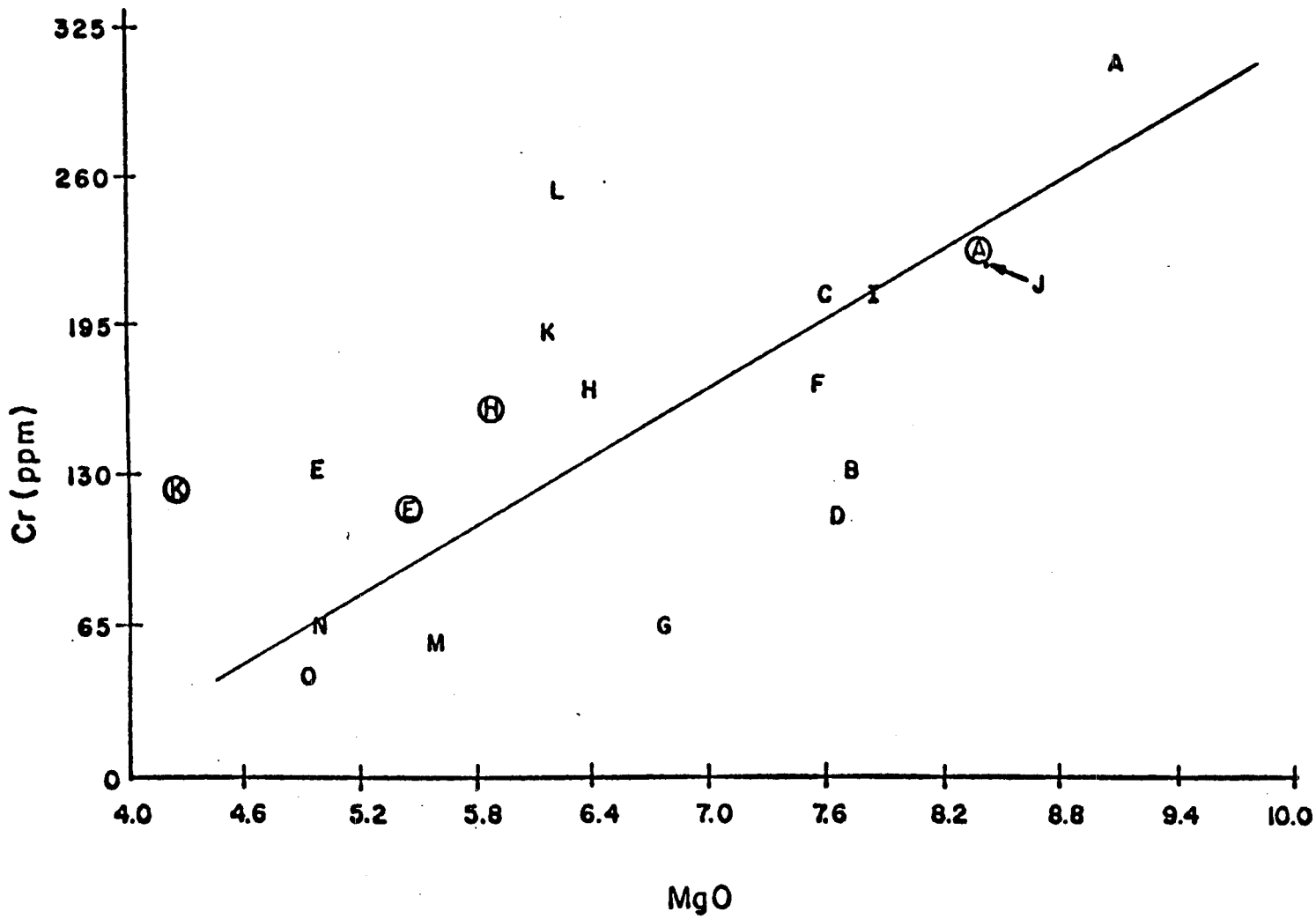
325
260
195
130
65
0
Cr (ppm)
4.0
4.6
5.2
5.8
6.4
7.0
7.6
8.2
8.8
9.4
10.0
MgO
A
L
K
H
C
I
F
B
D
E
N
M
O
G
J

TABLE VIII. -- Concentrations of Copper and Chromium in HGP-A Lavas, Kilauea East Rift Zone

	Elements	
Depth, m	Cu, ppm	Cr, ppm
0	90.5	42.0
186	125.6	67.8
287	116.8	35.9
287A	75.6	153.9
408	237.6	59.2
528	126.2	254.6
650	129.9	192.6
650A	NA	125.8
700	78.9	36.1
835	120.7	225.3
900	118.2	131.7
900A	97.2	143.4
976	135.6	205.3
1106	105.8	31.5
1203	105.9	166.1
1203A	109.6	159.4
1307	106.1	65.2
1402	118.9	178.7
1554	107.1	131.1
1554A	82.1	114.6
1673	110.8	113.4
1780	112.8	209.0
1882	110.0	133.0
1882A	48.2	209.5
1952	112.2	312.4
1952A	113.2	229.6

Note: "A" represents a highly altered sample from the same depth as the less altered samples.

NA = Not Analysed.

possible explanation for the chemical variations observed in HGP-A lavas is that drilling may have penetrated lavas of the ancient Kulani Shield, believed to lie between Mauna Loa and Kilauea and to be an independent volcanic series (Macdonald and Abbott, 1970). Chemical analyses of Kulani lavas do not exist, but to the southwest are rocks of the ancient Ninole Volcano (Fig. 1) which could be similar in age and composition to the Kulani lavas (G. Macdonald, personal communication, 1977). Analyses of the Ninole lavas have been published (Wright, 1971). The Ninole lavas are similar in composition to lavas penetrated in the lowermost portion of the well, namely samples A, B, C, and D (Table I). The possibility exists, therefore, that the deepest rocks penetrated by HGP-A are from the Kulani shield. Interfingering of Kilauea with Kulani lavas could explain the variations in composition of HGP-A lavas at intermediate depths, with only Kilauea lavas encountered in the upper portion of the well.

Conclusions

1. The effects of halmyrolysis on the chemistry of HGP-A lavas appear to be negligible, at least with respect to major elements.

2. Copper may have been effected by fractional crystallization, but the uniform concentrations observed today at deeper levels probably reflect the overprint of alteration which homogenized the distribution. Very altered samples are lower in Cu than their fresher counterparts from the same depth level, contrary to the findings of Thompson (1973) and Hart (1973) for halmyrolysis. Any alteration, therefore, must be due to groundwater or hydrothermal fluids. Variations in concentration near the surface probably reflect subaerial

weathering or groundwater alteration.

3. Chromium trends are variable; chromium appears to be slightly covariant with MgO implying that it might be carried by olivine as chrome-rich inclusions, but none are observed in olivine phenocrysts. The great variability, therefore, may reflect injection of "batches" of magma into the east rift zone, with various stages of fractional crystallization of pyroxene represented by variations in chromium concentration.

4. Three zones of lavas can be distinguished on the basis of chemical similarity. Four possible explanations are proposed.

a. The oldest (deepest) lavas are from the ancient Kulani Shield. Those of intermediate age (depth) represent interfingering of Kulani and Kilauea lavas. Lavas from the shallowest depths (youngest) are from Kilauea Volcano.

b. The observed variations represent chemical differentiation of the parent magma. Oldest (deepest) lavas are comparatively little differentiated, with changes in chemistry due to fractional crystallization only of olivine. The youngest lavas are differentiated by removal of clinopyroxene and feldspar also. The transition at intermediate depths is not smooth and could represent fluctuations in the amount of clinopyroxene and feldspar crystallization.

c. Magma "batches" are periodically injected into the east rift zone; the observed variations represent successive batches with decreasing magnesium content.

d. Alteration is responsible for selectively enriching or leaching certain oxides, due to variable temperatures of the water at different depths in the well.

II. PETROGRAPHY

Previous Investigations

Petrographic descriptions of Hawaiian rocks have been published by numerous investigators (see for example, Stearns and Macdonald, 1946; Macdonald, 1949; Macdonald and Katsura, 1964; and Macdonald, 1968). Macdonald (1969) described the petrology of very altered basalt cores from two drill holes on Midway Island. Grose and Keller (1976) briefly described the lavas from a 1261 m drill hole at the summit of Kilauea.

Materials and Methods

About three thin sections were made from each core by Western Petrographic, Tucson, Arizona. Modes were determined by point counting at least 200 points for one section from each core and visual modes were estimated for the remainder. A petrographic summary of each sample is contained in Appendix B. Sample numbers, where used, indicate the project name (HGP), the well (A), the core number (1-10), and the depth in meters (0-1962 m). For example, sample number HGP-A-4-676 is from Hawaii Geothermal Project, Well A, core 4, depth 676 m. More frequently samples are referred to as coming from "upper core 4." See Table IX for core depths.

Results and Discussion

Euhedral olivine phenocrysts are present in the first three cores. In cores 1 and 2 the grains are fresh with only minor corrosion and alteration to iddingsite around the edges; many are surrounded by a rim of second-generation olivine. Olivine phenocrysts comprise two to three per cent in cores 1 and 2 and average 0.6 mm in the largest

TABLE IX. -- Depth of Cores in Hawaii Geothermal Project Well-A

Core Number	Depth Below Surface, meters
1	133.5 - 134
2	317 - 320
3	425 - 428
4	674 - 677
5	871 - 874
6	1112 - 1115
7	1350 - 1353
8	1639 - 1642
9	1832 - 1835
10	1959 - 1962

dimension although a few grains exceed 1.3 mm. In the upper part of core 3 olivine phenocrysts are both more abundant (about six per cent), larger (maximum size about 2.2 mm), and more corroded and embayed than those found at shallower depths; but a few grains remain sharply euhedral. Thin rims of iddingsite and rims of opaque mineral grains are more pronounced on most phenocrysts, and most grains have second generation olivine surrounding the iddingsite. The phenocrysts exceed 2 mm in core 3 and grade in size into the groundmass. They decrease in abundance with depth in that core. Fresh olivine is not observed in deeper cores.

Plagioclase phenocrysts comprise one per cent or less in all cores except core 2 (four per cent), the bottom of core 4 (18 per cent), and core 9 (six per cent). Grains are euhedral to subhedral; a few are as great as 2 mm in the longest dimension but most are about 0.4 mm; in cores 2, 4, and 9 where they are abundant they grade in size into the groundmass. The Schuster method of extinction angle measurements indicates the phenocrysts have a compositional range of about An_{75-80}. Carlsbad twinning is common along with some albite twinning. Normal zoning occurs infrequently. Alteration to albite is first noted in core 7 and is extensive in core 10.

Phenocrysts of augite ($2V_z$ = 45-60°) occur in all rocks in varying amounts. They generally constitute less than one per cent, except in cores 1, 4 (lower half), 7, and 9 (lower portion) where they comprise five to eight per cent. Most grains are euhedral and average 0.3 mm in the largest dimension, although in the lower portion of core 4 grains reach a maximum of 2 mm. Normal and hourglass zoning occur in a few grains. Subophitic intergrowths and cumulophyric clusters of

augite and plagioclase occur locally in most thin sections. Most augite phenocrysts have been totally altered to actinolite in core 10.

The groundmass texture is generally intersertal although intergranular and glassy textures are not uncommon. The groundmass is composed of plagioclase, monoclinic pyroxene, magnetite, probably ilmenite, glass, and accessory apatite. Plagioclase is uniformly labradorite in composition (An_{60-68}), with most grains euhedral to subhedral and in random orientation. Microlite size averages 0.16 mm in the longest dimension but in a few coarser-grained rocks the groundmass plagioclase reaches a maximum of 0.5 mm. With increasing depth the groundmass becomes increasingly altered; montmorillonite, chlorite, actinolite, quartz, and an unidentified turbid material (altered glass ?) predominate. Vesicularity ranges from nonvesicular to about 30 per cent in the upper part of core 3. See Table X for estimated vesicularity and alteration in each thin section.

Several features of the samples are worth noting here. Two distinct types of changes appear to occur in the core lithologies. One type of change occurs where the core apparently penetrated an upper or lower chilled flow margin and a flow interior. For example, the upper portion of core 3 is highly vesicular (30 per cent) and the lower portion is less so. The texture also changes from intersertal to hyalopilitic. The sequence probably represents a flow interior transitional to a chilled lower margin.

The other type of change appears to occur across a lithologic contact between two units and is observed in cores 4 and 5. Core 4 apparently penetrated two contacts, or one lithologic contact and a transition of the core-3 type described above. The upper meter of core 4 is

TABLE X. -- Percentages of Vesicularity and Alteration in HGP-A Cores

Core	Depth, m	Per Cent Vesicularity	Degree Filled	Per Cent Alteration
1	133.5 (pc)	6	unfilled	none
	133.8	8	unfilled	none
	134	18	unfilled	none
2	318	13	unfilled	none
	319.5	13	unfilled	none
3	425.5 (pc)	31	slightly	trace
	427	25	slightly	trace
	428	20	slightly	trace
4	674.7	4	mostly	12
	675	28	mostly	14
	675.6	4	mostly	19
	676 (pc)	4	mostly	19
	677	0	--	10
5	871	20	mostly	45
	872	tr	completely	20
	874 (pc)	0	--	13
6	1112	0	--	23
	1112.8 (pc)	0	--	23
	1113	1	completely	23
	1115	6	completely	12
7	1350	0	--	50
	1351 (pc)	0	--	50
	1351.8	0	--	55
	1353	0	--	53
8	1640 (pc)	0	--	37
	1640.4	0	--	37
	1642	1	completely	37
	1642.5	2	completely	45
9	1833.3 (pc)	0	--	87
	1834	0	--	80
	1835	0	--	75
10	1959.8 (pc)	tr	mostly	84
	1959.9	12	mostly	96
	1961	6	mostly	95

Note: (pc) designates those thin sections point counted; all other modes were visually estimated.

generally fine-grained and vesicular with nearly all phenocrysts altered to montmorillonite and with opaque grains rimming numerous vesicles. Below that a glassy contact is penetrated by sample HGP-A-4-675.2 where fresh and altered phenocrysts occur together in a matrix of brown and black glass. Below the contact all vesicles are surrounded by a thick rim of black glass and the rock is more coarse-grained. Plagioclase phenocrysts comprise nearly 18 per cent in this portion and range in size from 0.1 to 2 mm. Augite phenocrysts also attain a maximum size of 2 mm. The lowermost meter is again fine-grained, but nonvesicular and less altered. The upper portion of core 5 has numerous vesicles, wholly to partially filled with secondary alteration products and is more extensively altered than the lower part. Below the contact the rock is nonvesicular with a distinctly hyalopilitic texture. In hand specimen even the lower portion of core 5 displays a very glassy appearance. The thickness of this very glassy section is not completely understood. That cores 4 and 5 have penetrated lithologic contacts is further supported by mercury analyses showing that Hg contents vary between the top and bottom of each core by factors of four to five (S. Siegel, personal communication, 1976).

The percentage of alteration in each core varies, probably depending on glass content, permeability, and temperature of the water at different depths in the well. See Table X.

Conclusions

1. The cores represent less than two per cent of the rocks penetrated by the well. This must be kept in mind in making further conclusions.

2. The well appears to have penetrated a series of subaerial lava flows and submarine pillow (?) basalts on the basis of vesicularity: cores 1 through 4, highly to moderately vesicular; cores 5 through 10, slightly to nonvesicular.

3. Core 6 is equigranular, nonporphyritic, and virtually nonvesicular. It is less altered than cores 5 and 7, and may be a dike or a sill-like intrusion.

4. The coarse-grained portions of cores probably represent the interiors of thick flow units.

5. Based on filled vs. unfilled fractures and vesicles, three zones of permeability can be identified: cores 1 through 5 (0 - 871 m), highly permeable; cores 6 through 9 (1113 - 1835 m), poorly permeable; core 10 (1952 m), moderately permeable.

6. A reliable estimate of porosity cannot be made on the basis of vesicles alone in Hawaiian lavas.

III. HYDROTHERMAL ALTERATION

Previous Investigations

Chemical alteration of Kilauea basalts due to gases escaping along faults (Stearns and Macdonald, 1946) and the present-day formation of palagonite in Kilauea caldera (Hay and others, 1969) have been described. Fujishima and Fan (1977) studied hydrothermally altered basalts of the Kailua Volcanic Series, Oahu, and described both vertical and horizontal zones of clay mineral alteration. Hydrothermal alteration of Icelandic basalts in high- and low-temperature geothermal fields has been recently summarized (Kristmannsdóttir, 1976).

Materials and Methods

A. Sample Selection. Cutting samples were selected at 50 m intervals for the length of the well. Whole-rock splits were taken from each sample bag to assure homogeneity. The cutting chips were cleaned for 15 minutes in an ultrasonic cleaner and ground for 20 minutes in a Spex ball mill. Powdered samples were stored in clean glass vials.

B. Sample Preparation. Specimens were prepared for X-ray examination by firmly loading an aluminum specimen holder from the back, with the surface to be exposed to the X-rays face down on rough filter paper to insure random orientation (Hutchinson, 1974). A petrographic slide was taped to the back of the specimen holder after loading to prevent loss of sample.

Samples were X-rayed with a Norelco diffractometer, type number 12215/A, manufactured by Philips Electronic Instruments. Copper K_α radiation with a Ni filter was used at 35 kV and 20 mA. The following instrument settings were used:

Chart speed	one half inch per minute
Goniometer speed	1° 2θ per minute
Time constant	4 seconds
Rate meter	10^2
Rate meter multiplier	5

C. Analytical Methods. A whole-rock X-ray diffractogram was made of HIG S-2, a fresh Kilauea tholeiite described by Macdonald (1972). Tracings of HGP-A samples were compared with this tracing for identification of the principal constituents, and d-spacings were verified in the Powder Diffraction File. Also, single and double-mineral X-ray diffractograms of the minerals anticipated in the HGP-A rocks were borrowed where available (G. McMurtry, 1976) or made for comparison with the diffractograms of samples. Peaks which could not be identified by this method were looked up in the Powder Diffraction Index. Selected mineral separates of only three samples were X-rayed. It was planned to do many more separates for more definitive identification of zeolites, chlorite, and the various clay minerals, but the X-ray diffraction tube burned out in November, 1976, and has not been replaced as of this writing.

Results and Discussion

The occurrence of secondary minerals identified in HGP-A lavas is shown in Figure 16 along with two temperature profiles. The profile indicated by the heavy solid line was taken May 2, 1976, 97 hours after mud recirculation had stopped in the well. Solidification of mud prevented the probe from dropping deeper in the well. A maximum temperature of 358°C (dash-dot profile) was measured immediately after flashing on July 22, 1976, at the bottom of the well; but it is believed that

Figure 16. The occurrence of hydrothermal alteration products with depth in the well, HGP-A lavas, Kilauea east rift zone. See text for explanation of temperature profiles.

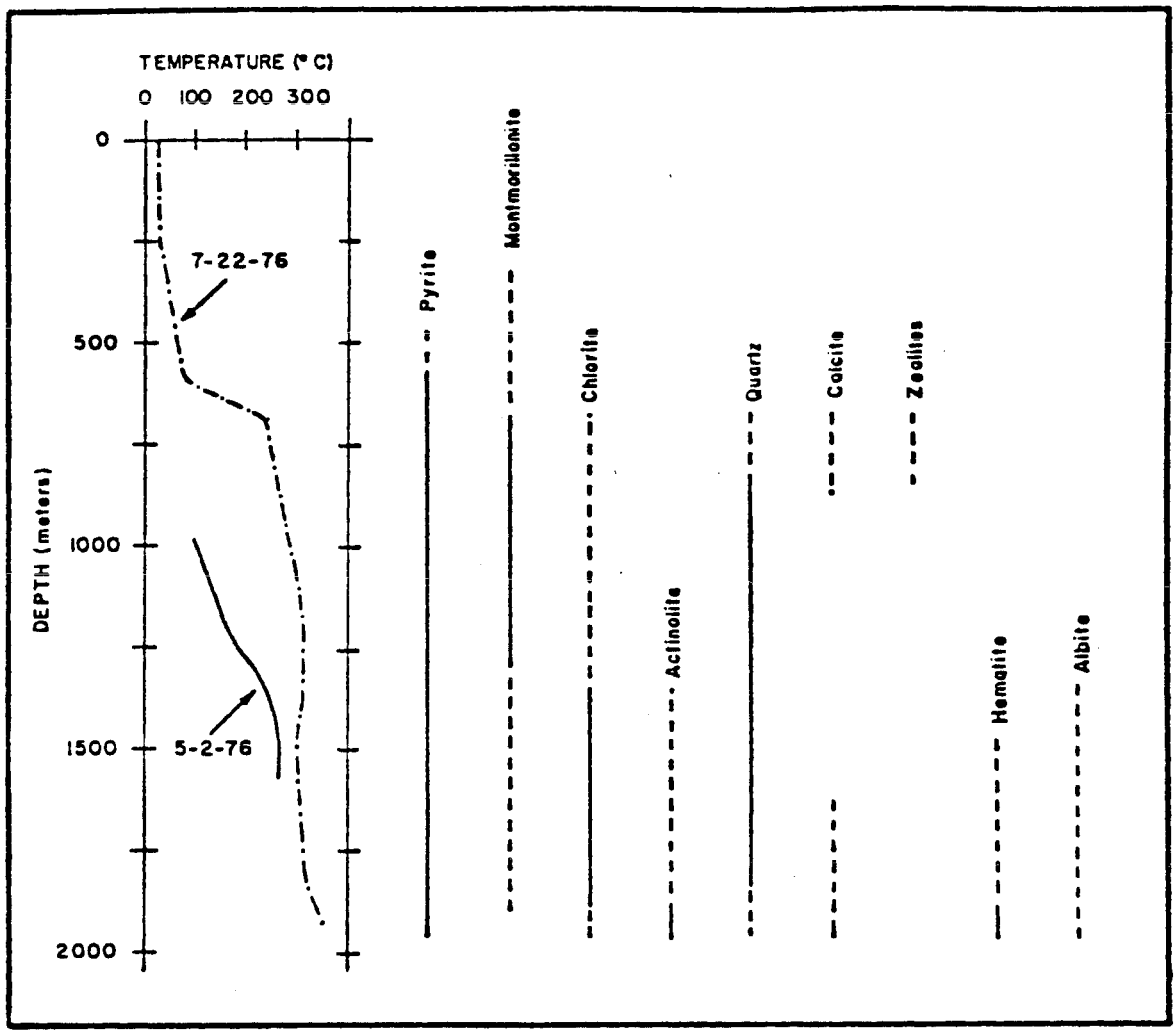
TEMPERATURE (° C)
0 100 200 300
DEPTH (meters)
0
500
1000
1500
2000
7-22-76
5-2-76
Pyrite
Montmorillonite
Chlorite
Actinolite
Quartz
Calcite
Zeolites
Hematite
Albite

drilling disturbed the thermal regime and that pre-drilling equilibrium had not been reestablished in the well. Fresh water, thought to represent water pumped into the well during drilling (G. Macdonald, personal communication, 1977), is probably still being pumped out during tests, as of this writing. Therefore, relating a pre-drilling, equilibrium temperature profile to the observed secondary mineral assemblages is impossible at the present time. Secondary mineral assemblages in Icelandic geothermal fields are believed to be predominantly temperature dependent (Kristmannsdóttir, 1975). However, the changeover in assemblage from montmorillonite to chlorite in HGP-A lavas does not occur at the same temperature as it does in Iceland. It appears to occur at a higher temperature. Both fields are in predominantly basaltic lavas. Therefore, other factors such as slightly acidic water, rock permeability, or glass content of lavas must be more significant in Hawaii than they are in Iceland.

The occurrence of the following secondary minerals was observed by at least one of these methods: in hand specimen, in thin section, or by X-ray diffraction.

1. Montmorillonite. Traces of montmorillonite rimming a few olivine phenocrysts is first noted at about 318 m. By 675 m the montmorillonite is present interstitially and as pseudomorphs after olivine. It increases in abundance with depth to about 1300 m in this same mode, and then decreases as chlorite becomes the dominant alteration mineral. An observation made in most high-temperature geothermal wells in Iceland (Tómasson and Kristmannsdóttir, 1972) is that the transition from montmorillonite to chlorite as the dominant alteration product occurs in the temperature range of 200-230°C, but as noted above our findings are not

consistent with theirs. Montmorillonite is not observed below 1894 m.

A mineral separate from 726 m was X-rayed, heated for one hour at 300°C, and X-rayed again (Hutchinson, 1974). A peak shift in d-spacing from 15.04 to about 9.6 confirms that the identification of montmorillonite in thin section by general appearance, low relief, and high birefringence (~0.030) is correct, at least at that depth.

2. Chlorite. Chlorite is found locally at 675 m and occurs sporadically to 1350 m where it replaces montmorillonite as the dominant alteration mineral. It occurs interstitially, filling vesicles and fractures, as pseudomorphs, and replacing actinolite in the centers of pseudomorphs of actinolite after augite and olivine in core 10. Chlorite is present to the bottom of the well but is superceded by actinolite as the principal alteration product at 1894 m. By 1959 m chlorite is a minor constituent only.

Because optical identification is tentative and because it was not possible to perform heating and glycolating operations on samples for definitive identification of clay minerals, the occurrence of chlorite was "confirmed" mainly by correlating the quantity of the mineral optically identified as "chlorite" with the height of the X-ray diffraction peak (d-spacing = 7.08) identified as representing chlorite. The correlation was good in that where abundant chlorite was observed in thin section, peak height was high; where chlorite was minor or absent, peak height was small or absent.

3. Actinolite. Actinolite is found at 1350 m and is sporadic to 1894 m. From this depth to the bottom of the well it is the dominant alteration product. It occurs as pseudomorphs after augite and olivine and as a groundmass replacement along with quartz, magnetite, and hematite.

4. Calcite. Between 675 m - 875 m and again between 1835 m - 1962 m, calcite is found in thin section as a minor constituent partly filling some vesicles. It is also observed lining fractures in hand specimens of cores 8, 9, and 10. Euhedral crystals in fractures in core 10 indicate that the rock is not completely sealed at that depth. Calcite is nowhere abundant enough to be detected by whole-rock X-ray diffraction.

5. Zeolites. Zeolites of unidentified species are found between 675 m - 875 m; they appear along a flow margin at 675 m and lining vesicles there and in other samples. At 875 m an isotropic species is found; it is possibly analcite (K. Pankiwskyj, personal communication, 1977). A fibrous, isotropic-appearing zeolite is found at 876 lining some vesicles. Zeolites do not appear to occur at greater depths in the well where higher temperatures prevail.

6. Opaque Minerals. Magnetite is found in varying amounts throughout the section. It occurs as primary euhedral crystals, secondary skeletal grains, by-product dust, and as a filling of vesicles along with quartz and clay minerals. At 1480 m hematite is found by X-ray diffraction and it occurs sporadically to a depth of 1894 m where it exceeds magnetite and becomes the dominant opaque mineral to the bottom of the well. This occurrence of hematite coincides with that of actinolite, possibly indicating higher temperatures at that depth, a more hydrous regime, or a different type of alteration. Pyrite is first observed in cutting chips at 485 m and is present in varying amounts throughout the section. In shallow cores ilmenite is found in thin section, but with increasing depth and alteration it is not recognized.

7. Quartz. Minor amounts of quartz are first found filling

vesicles at about 675 m. It becomes increasingly abundant with depth to about 1835 m and then decreases somewhat. If a different type of alteration is operative below 1835 m or if temperatures at that depth are very high, thermal fluids could be removing SiO_2. The high silica content of thermal waters currently issuing from the well, 600 ppm (P. Yuen, personal communication, 1977), seem to bear this out. Another possibility, however, is that the host rock was initially low in silica. In sample HGP-A-8-1642.5 quartz appears to be replacing plagioclase but this is not observed in other samples.

8. Albite. Albite or a very Na-rich plagioclase is found at 1350 m, increasing with depth in the well. It is a result of the alteration of the primary labradorite feldspar phenocrysts.

Conclusions

1. Beneath a zone of unaltered lavas, high temperatures and hydrothermal fluids have created three altered zones, each marked by the dominance of a particular mineral (Fig. 16). The uppermost altered zone, 675 m - 1300 m, is characterized by montmorillonite with minor calcite, quartz, one or more zeolites, and chlorite. Vesicles in this zone are only partly filled with secondary minerals. The second hydrothermal zone, 1350 m - 1894 m, begins with the occurrence of extensive chlorite replacing montmorillonite as the dominant alteration product. Quartz, actinolite, and montmorillonite are the accessory secondary minerals. All vesicles and fractures are completely filled within this zone. The third zone of alteration is observed beginning in core 9, 1894 m, and is dominant in core 10, 1959 m. Actinolite is the dominant mineral; chlorite, quartz, opaque grains are the accessory alteration

products. Both the degree and type of alteration found in core 10 are distinct from those encountered in the lavas above. It is far more extensive than alteration at shallower depths although it is beginning to be seen in core 9. The mineral assemblage resembles that found in greenschist facies metamorphism and reflects higher pressure and probably higher temperature than the alteration to clay minerals at higher levels. In addition all fractures and vesicles in cores 6 through 9 are completely sealed with secondary minerals, but those in core 10 are only partly filled.

From these observations, realizing that the cores constitute less than two per cent of the well, it could be concluded that the first zone of hydrothermal alteration, between 675 m - 1350 m, is relatively permeable, allowing groundwater coming from or heated by conduction from greater depths to circulate freely. The zone between 1350 m - 1959 m is relatively impermeable, a self-sealed rock capping the geothermal reservoir. Below 1959 m is the geothermal reservoir itself, a moderately permeable zone allowing thermal fluids to move with relative ease. The decrease in quartz in this zone and the high concentration of silica found in thermal waters issuing out at the surface indicate that the thermal waters may originate in this zone. The heat source for these thermal fluids could be one or more of the following possibilities.

1. A magma-holding reservoir within the east rift zone, periodically fed by lateral injections of magma from the main reservoir beneath the summit of Kilauea (Wright and Fiske, 1971).

2. The heat of reaction due to the alteration of primary minerals to secondary ones, an exothermic reaction (Hart, 1973).

3. An extensive zone of slowly-cooling dikes beneath the east rift zone, renewed at the time of each east-rift eruption.

4. Large, slowly-cooling stocks within the east rift zone, emplaced periodically by lateral injection from the summit reservoir, suggested by the presence of nearby pit craters.

The possibility exists that one or more of these sources contribute to the overall heat observed in HGP-A. Petrographic evidence by Wright and Fiske (1971) presents a strong argument in favor of a magma-holding reservoir within the east rift zone. The presence of extensive dikes within the east rift zone is supported by geologic and geophysical evidence (A. Furumoto, personal communication, 1977). It seems probable, therefore, that large batches of magma confined by some structure are the most likely heat source. If this is true and new batches are injected periodically, it seems likely that the heat source is permanent and that useable geothermal energy will be a reality in Hawaii.

2. Kristmannsdóttir (1975) suggested that the appearance of amphibole at the highest temperatures (nearly 300°C) in high-temperature geothermal areas in Iceland might mark the beginning of a previously unsuspected amphibole zone below the chlorite-epidote zone. Since HGP Well-A is deeper and appears to be hotter than Icelandic wells, the occurrence of abundant actinolite in core 10 seems to confirm her suspected amphibole zone.

3. The changeover temperature from a montmorillonite zone to a chlorite zone in HGP Well-A is greater than the temperature range at which the same transition happens in Icelandic wells. Therefore, more acidic water, rock permeability, or glass content of lavas must be more significant in Hawaii than in Iceland to account for this observation.

Appendix A

Experimental Methods

The elemental copper spectrum was beamed through an air-acetylene flame, amplified, and recorded on a Perkin-Elmer Model 165 Recorder. Scale expansion was X10 and noise suppression was X1. A Boling triple-slot air-acetylene burner was used. Samples and standards were aspirated into the flame in the following order: low Standard, Sample A, high Standard, Sample A, low Standard, Sample A, high Standard. Peak heights of each solution were averaged. Sample concentrations were then determined from a working curve constructed by plotting peak height against concentration of the two known standards which bracketed the sample. It was believed that determining sample concentrations from segments of a curve rather than from one integrated curve would produce more accurate data as the integrated curve would smooth out the segments, reducing accuracy.

The elemental chromium spectrum was beamed through a nitrous oxide-acetylene flame to eliminate chemical interferences of Ni and Fe (Robinson, 1975). A 5-cm single-slot nitrous oxide-acetylene burner was used. Samples and standards were aspirated into the flame in the order described above for copper. Working curves for chromium were computed by the Model 603 spectrophotometer on the basis of known standards programmed into the instrument. Sample concentrations were read directly from a digital display. Because background noise was excessive, sometimes as great as $\pm$ 0.057 μg/ml, it was averaged between readings and subtracted or added from sample concentrations where it was positive or negative, respectively.

In order to bracket each sample with standards, a trial run of

each element was made prior to the final analysis to estimate sample concentrations. A baseline for each element was determined continuously by aspirating distilled and deionized water. Initially an aqueous solution containing HF, H_3BO_3, and aqua regia in the same concentrations as in the samples and standards was used, but there was no apparent difference between this and the water baseline so the latter was used in all final determinations.

Trial analyses of rubidium, nickel, cobalt, barium, and strontium were made but reliable data were not obtained for several reasons. (1) Rubidium concentrations, usually less than ten ppm in Hawaiian lavas (Hubbard, unpublished Ph.D. dissertation, 1967) were too low to be detected in the sample solutions as prepared. (2) Nickel is subjected to chemical interferences from Cr and Fe which can be reduced or eliminated in a nitrous oxide-acetylene flame (Robinson, 1975). The background noise, however, was exorbitant, as great as $\pm$ 0.76 μg/ml, and could not be eliminated in this flame. Data were inaccurate in the air-acetylene flame. (3) Cobalt needs a deuterium arc background correction (V. Greenberg, personal communication, 1977). When the reference Co beam is replaced by the deuterium beam there is no longer a reference for the background. Erratic energy from the Co lamp caused the baseline to drift continuously. It was concluded that the available Co lamp was unstable (C. Fein, personal communication, 1977).

Appendix B

Detailed Summary of Petrography

Core-Depth, m	Summary
1-133.5	Vesicular and porphyritic with intergranular texture. Phenocrysts up to 1.2 mm in size of 6% augite ($2V_z$ = 50°), 2% olivine, and <1% plagioclase (An_{80}). Groundmass is 46% pyroxene, 22% plagioclase (An_{60}), 17% opaques and 6% vesicles. Olivine phenocrysts are slightly corroded with minor iddingsite and secondary olivine surrounding a few grains. Plagioclase microlites average 0.1 mm in length.
1-133.8	Similar to above except vesicles are more numerous, 8%; augite and olivine phenocrysts are less abundant.
1-134	Similar to above except vesicles are more numerous, 18%.
2-318	Vesicular and porphyritic with intersertal texture. Phenocrysts are 2.5% plagioclase, 2% augite ($2V_z$ = 45-50°), and <1% olivine. Groundmass is black glass, plagioclase (An_{68}), pyroxene, opaques, and vesicles. The rock is somewhat coarse grained.
2-319.5	Vesicular and aphanitic with intersertal texture. Local patches up to about 1 mm across are almost entirely black glass. Black glass constitutes 22%; plagioclase (An_{65}), 20%; pyroxene, 16%; vesicles, 13%; opaques, 27%. Rare microphenocrysts of plagioclase and clinopyroxene observed. Plagioclase microlites average 0.16 mm.
3-425.5	Vesicular and porphyritic with intersertal texture. Vesicles are pahoehoe type. Phenocrysts are 6% olivine, less than 1% each augite ($2V_z$ = 55°) and plagioclase (An_{75}). Groundmass is 31% vesicles, 17% pyroxene, about 15% each black glass, opaques, and plagioclase (An_{62}). Olivine phenocrysts are corroded and embayed and many are surrounded by secondary magnetite grains and/or slight iddingsite. Plagioclase microlites average about 0.16 mm in length.
3-427	Similar to above except vesicles, 25%, and olivine, <1%, are less abundant; and vesicles are less regular. Irregular, finer-grained patches appear to have the same mineral composition as the rest of the rock.
3-428	Vesicular and porphyritic with a vitrophyric texture. Plagioclase and augite comprise less than 1% each and occur in a few cumulophyric clusters. Vesicles are about 20%; groundmass, 79%. A very few vesicles are filled with a greenish-brown material (montmorillonite ?).
4-674.7	Vesicular and porphyritic with intergranular texture. Phenocrysts are 4.5% montmorillonite (determined by X-ray) after olivine, 1% augite ($2V_z$ = 45°), 1% plagio-

clase. Groundmass is 27% plagioclase (An_{60}), 53% clinopyroxene, 6% opaques, 4% vesicles, and 4% interstitial montmorillonite (altered glass ?). Zeolites, quartz, and chlorite comprise less than 1% each. Plagioclase microlites average 0.16 mm in length.

4-675 Similar to above except more vesicular, 28%, and slightly more montmorillonite after olivine, 5.6%, and more opaque grains. Calcite, less than 1%, partially filling some vesicles. Fibrous isotropic zeolite, 2%, and opaque grains lining many vesicles.

4-675.6 Vesicular and porphyritic with intersertal texture. Plagioclase phenocrysts are larger, up to 2.5 mm, than in sample 4-675; they are also more abundant, 30%, and seriate. Augite ($2V_z$ = 45-50°) and montmorillonite after olivine, about 7% each. Groundmass is more altered than above with abundant secondary magnetite, montmorillonite and glass (?). Alteration around vesicles is greater than in sample 4.675. Character is totally different from other rock in core 4 above.

4-676 Similar to above. One subophitic augite is nearly 2mm in size.

4-677 Nonvesicular and less altered than above, but alteration is of the same type. Augite ($2V_z$ = 45-50°) phenocrysts, 2%, and montmorillonite after olivine, 1%, are less. Plagioclase phenocrysts about 22%. Two olivine phenocrysts are not completely replaced by montmorillonite. Minor quartz and chlorite (?) filling one vesicle each.

5-871 Vesicular and porphyritic with intersertal texture. Phenocrysts are <1% augite ($2V_z$ = 45-50°). Vesicles nearly completely filled with montmorillonite, zeolite, calcite and quartz. Secondary magnetite surrounds most vesicles. Groundmass is fine-grained plagioclase (An_{68}) 33%; turbid, fibrous material (?), 37%; montmorillonite and opaques, 12% each; quartz, 4%; clinopyroxene, 2%; zeolite, less than 1%.

5-872 Vesicular but all filled. Very fine grained; plagioclase microlites average 0.09 mm in length, and vesicles, 0.16 mm. Montmorillonite pseudomorphs, <1%. Augite (0.5 mm), 2%. Banding is observed, due to increased alteration and glass. Fractures filled with quartz, opaques, and montmorillonite. Variolitic groundmass is predominantly plagioclase and a turbid fibrous material. Plagioclase laths are in radiating and sheave-like groups.

5-874 Nonvesicular and porphyritic with intersertal texture. Phenocrysts are less than 1% each plagioclase (An_{77}) and augite ($2V_z$ = 50-55°). Groundmass consists of 45% black glass and opaques which are indistinguishable, 25% pyroxene, 19% plagioclase (An_{64}), 10% montmorillonite and traces of calcite and chlorite (?). Rock is less altered than speciman 5-872, above.

6-1112 Nonvesicular and nonporphyritic with intersertal texture. Microphenocrysts of plagioclase, 1 only; augite, several. Plagioclase microlites (An_{80}) comprise 33%, average 0.2 mm. Clinopyroxene, 35%; montmorillonite (?) 13%; opaques, 9%; quartz, 6%; and traces of chlorite.

6-1112.8 Similar to specimen 6-1112, above.

6-1113 Similar to above except vesicles, about 1%, filled with quartz, and euhedral magnetite absent. Secondary skeletal pyrite is present. The groundmass shows a tendency toward variolitic texture.

6-1115 Vesicular and prophyritic with glassy texture. Vesicles 6%, are filled with montmorillonite predominantly, some quartz and chlorite. Phenocrysts are plagioclase, 1%, and augite, 2%, in a matrix of microcrystalline plagioclase laths and secondary pyrite (?) in black glass. Plagioclase phenocrysts are slightly altered along fractures to montmorillonite (?). Montmorillonite pseudomorphs, 3%, are present.

7-1350 Nonvesicular with scant phenocrysts of augite ($2V_z = 45^o$) and plagioclase, less than 1% each. Texture is glassy with abundant secondary magnetite, plagioclase and turbid material (altered glass ?). Large grains of pyrite, 0.35 mm average, occur in the groundmass, filling fractures with chlorite, quartz and montmorillonite. Some fractures are filled with what appears to be glass.

7-1351 Nonvesicular and porphyritic with intersertal texture. Phenocrysts are 8% augite ($2V_z = 45^o$) and 2% plagioclase (An_{78}) occurring principally in cumulophyric clusters. The feldspar shows only traces of alteration. Groundmass is 20% plagioclase (An_{65}), 20% opaques, 27% turbid material, 15% clinopyroxene, and 5¢ montmorillonite, with traces of quartz and chlorite. The opaques include much pyrite.

7-1351.8 Nonvesicular and porphyritic with intersertal texture; finer-grained than specimen 7-1351, above. Phenocrysts are about 2% augite ($2V_z = 45^o$) and less than 1% plagioclase. Chlorite pseudomorphs occur and extensive chlorite, quartz and pyrite fill large fractures and former crushed zone completely. Chlorite occurs interstitially with turbid material, plagioclase, quartz and opaques. Actinolite is first observed with chlorite in pseudomorphs. Plagioclase is altering to albite or Na-rich feldspar.

7-1351 Nonvesicular and porphyritic with intersertal texture. Phenocrysts of augite ($2V_z = 45\text{-}50^o$), 6%; partly altered plagioclase, 5%. Groundmass is turbid material (altered glass ?), 29%; plagioclase, 20%; clinopyroxene, 14%; chlorite, 11%; opaques, 9%; and quartz, 7%. Fractures are completely filled with quartz.

8-1640 Nonvesicular and porphyritic with intersertal texture. Phenocrysts are augite ($2V_z = 50\text{-}55^o$), <1%, and plagio-

clase, some with normal zoning, altering to albite, 2%. Groundmass is plagioclase, 33%; clinopyroxene, 24%; turbid material, 19%; chlorite, 10%; opaques, 8%; and quartz, 5%. This rock is somewhat coarse-grained with plagioclase phenocrysts reaching maximum size of 2.2 mm and groundmass plagioclase averaging 0.5 mm. The opaques are partly pyrite.

8-1640.4 Similar to specimen 8-1640, above.

8-1642 Similar to above except vesicles, 1%, are filled with quartz; groundmass is slightly less coarse-grained; minor actinolite appears with some chlorite.

8-1642.5 Similar to above only vesicles, about 2%, are filled with quartz, pyrite grains, chlorite and actinolite. Quartz and turbid material are more abundant in the groundmass, and plagioclase appears to be replaced by quartz in a few instances.

9-1833.3 Nonvesicular and porphyritic with intersertal texture. Phenocrysts are about 3% plagioclase and 2% clinopyroxene. Calcite, chlorite and actinolite (less than 1% each), quartz, 3%, opaques, 12%, and montmorillonite (?) are present as alteration products of phenocrysts and in the groundmass. Groundmass, about 80%, is principally turbid brown material and opaques, and is very fine-grained. Clinopyroxene is corroded. The opaques are mostly magnetite and/or ilmenite, with larger pyrite grains along fractures.

9-1834 Nonvesicular and porphyritic with intersertal texture. Phenocrysts are more abundant: 7% plagioclase (An_{75}), and 3% augite ($2V_z = 45^o$). Highly elongate grains of olivine have been wholly altered to montmorillonite (?). Skeletal magnetite and other opaque grains are more abundant. Groundmass is more coarse-grained; feldspar laths average 0.26 mm in length.

9-1835 Similar to specimen 9-1834, above; slightly less turbid material in groundmass, and more plagioclase.

10-1959.8 Vesicular and porphyritic with intersertal texture. Phenocrysts are less than 1% each altered plagioclase, 2.2 mm in length, and chlorite and actinolite after augite and olivine. Groundmass is fine grained actinolite, 31%; turbid material, 21%; opaques, 19%, plagioclase, 13%; quartz, 11%; and chlorite, 6%. Vesicles are less than 1%.

10-1959.9 Vesicular and porphyritic with turbid, fibrous-green groundmass. Vesicles, about 12% are filled with pyrite grains, chlorite, and quartz, but some only partly. All fractures are not completely filled. Actinolite pseudomorphs after augite and olivine; some centers have been altered from actinolite to chlorite.

10-1961 Similar to 10-1959.9, above. Quartz and opaque grains are partly filling vesicles.

LITERATURE CITED

Berman, E.R., 1975, Geothermal energy, Noyes Data Corp., Park Ridge, N.J., 336 p.

Bowen, R.W., 1971, Graphic normative analysis program: National Technical Information Service, PB 206 736, Springfield, Va. 22151, 80 p.

Buckley, D.E. and Cranston, R.E., 1971, Atomic absorption analysis of 18 elements from a single decomposition of aluminosilicate: Chem. Geol., v. 7, p. 273-284.

Ellis, A.J., 1969, Geochemistry in volcanic hydrothermal areas, in Khitarov, N.I., ed., Problems in geochemistry: Washington, D.C., U.S. Dept. of the Interior and National Science Foundation, 372 p.

Flanagan, F.J., 1973, 1972 values for international geochemical reference samples: Geochima. et Cosmochima. Acta, v. 37, p. 1189-1200.

Fujishima, K. and Fan, P.F., 1977, Hydrothermal mineralogy of Keolu Hills, Oahu, Hawaii: Am. Mineralogist (in press).

Grose, L.T. and Keller, G., 1976, Petrology of deep drill hole, Kilauea volcano: EOS Trans. Am. Geophys. Union [abstr.], v. 57, p. 1017.

Gunn, B.M., 1971, Trace element partition during olivine fractionation of Hawaiian basalts: Chem. Geol., v. 8, p. 1-13.

Hart, R.A., 1973, A model for chemical exchange in the basalt-seawater system of oceanic layer II: Can. J. Earth Sci., v. 10, p. 799-816.

Hart, S.R., 1973, Submarine basalts from Kilauea rift, Hawaii: nondependence of trace element composition on extrusion depth: Earth Planet. Sci. Lettr., v. 20, p. 201-203.

Hay, R.L., Burns, L.K., and Drake, R., 1969, Palagonitic alteration along steaming cracks in Kilauea caldera, Hawaii: Geol. Soc. Am. Abs. with Programs for 1969, Part 7, p. 92-93.

Hubbard, N.J., 1967, Some trace elements in Hawaiian lavas (Ph.D. dissert.]: Honolulu, Univ. Hawaii, 123 p.

Hutchison, C.S., 1974, Laboratory handbook of petrographic techniques: John Wiley & Sons, New York, 527 p.

Koenig, J.B., 1973, Worldwide status of geothermal resources development, in Kruger, P. and Otte, C., eds., Geothermal energy: Stanford, Stanford Univ. Press, 360 p.

Kristmannsdóttir, H., 1975, Hydrothermal alteration of basaltic rocks in Icelandic geothermal areas, in Second UN symposium on the development and use of geothermal resources: San Francisco Proceedings, Lawrence Berkeley Lab, Univ. Calif., p. 441-445.

Macdonald, G.A., 1949, Petrography of the island of Hawaii: U.S. Geol. Surv. Prof. Paper 214-D, p. 51-96.

_____ 1968, Composition and origin of Hawaiian lavas: Geol. Soc. America Memoir, no. 116, p. 477-522.

_____ 1969, Petrology of the basalt cores from Midway Atoll: U.S. Geol. Surv. Prof. Paper 680-B, 10 p.

_____ 1973, Geological prospects for development of geothermal energy in Hawaii: Pacific Sci., v. 27, p. 209-219.

_____ and Katsura, T., 1964, Chemical composition of Hawaiian lavas: J. Petrol., v. 5, p. 82-133.

_____ and Abbott, A.T., 1970, Volcanoes in the sea: the geology of Hawaii: Honolulu, Univ. Hawaii Press, 441 p.

Moore, J.G., 1965, Petrology of deep-sea basalt near Hawaii: Am. J. Sci., v. 263, p. 40-52.

Stearns, H.T. and Macdonald, G.A., 1946, Geology and ground-water resources of the island of Hawaii: Hawaii Div. of Hydrography, Bull. 9, 363 p.

Thompson, G., 1973, A geochemical study of the low-temperature interaction of sea-water and oceanic igneous rocks: EOS Trans. Am. Geophys. Union, v. 54, p. 1015-1019.

Tómasson, J. and Kristmannsdóttir, H., 1972, High temperature alteration minerals and thermal brines, Reykjanes, Iceland: Contr. Mineral. and Petrol., v. 36, p. 123-134.

Turekian, K.K., 1963, The chromium and nickel distribution in basaltic rocks and eclogites: Geochim. et Cosmochim. Acta., v. 27, p. 835-846.

Wright, T.L., 1971, Chemistry of Kilauea and Mauna Loa lava in space and time: U.S. Geol. Surv. Prof. Paper 735, 40 p.

_____ and Fiske, R.S., 1971, Origin of differentiated and hybrid lavas of Kilauea volcano, Hawaii: Jour. of Petrol., v. 12, p. 1-65.

_____ 1971, Fink inorganic index to the powder diffraction file: Joint Committee on Powder Diffraction Standards, Swathmore, Pa., 1084 p.

_____ 1973, Analytical methods for atomic absorption spectrophotometry: Perkin-Elmer Corp., Norwalk, Conn., unpaginated.